JACS
JOURNAL OF THE AMERICAN CHEMICAL SOCIETY
Article
pubs.acs.org/JACS

Organocatalytic Conjugate-Addition Polymerization of Linear and Cyclic Acrylic Monomers by N-Heterocyclic Carbenes: Mechanisms of Chain Initiation, Propagation, and Termination

Yuetao Zhang,[†] Meghan Schmitt,[†] Laura Falivene,[‡] Lucia Caporaso,[‡] Luigi Cavallo,*[,§] and Eugene Y.-X. Chen*[,†]

[†]Department of Chemistry, Colorado State University, Fort Collins, Colorado 80523-1872, United States

[‡]Dipartimento di Chimica e Biologia, Università di Salerno, I-84084, Fisciano, Italy

[§]Physical Sciences and Engineering Division, Kaust Catalysis Center, King Abdullah University of Science and Technology (KAUST), Thuwal 23955-6900, Saudi Arabia

Supporting Information

ABSTRACT: This contribution presents a full account of experimental and theoretical/computational investigations into the mechanisms of chain initiation, propagation, and termination of the recently discovered N-heterocyclic carbene (NHC)-mediated organocatalytic conjugate-addition polymerization of acrylic monomers. The current study specifically focuses on three commonly used NHCs of vastly different nucleophilicity, 1,3-di-*tert*-butylimidazolin-2-ylidene (I^{t}Bu), 1,3-dimesitylimidazolin-2-ylidene (IMes), and 1,3,4-triphenyl-4,5-dihydro-1*H*-1,2,4-triazol-5-ylidene (TPT), and two representative acrylic monomers, the linear methyl methacrylate (MMA) and its cyclic analog, biomass-derived renewable γ-methyl-α-methylene-γ-butyrolactone (MMBL). For MMA, there exhibits an exquisite selectivity of the NHC structure for the three types of reactions it promotes: enamine formation (single-monomer addition) by IMes, dimerization (tail-to-tail) by TPT, and polymerization by I^{t}Bu. For MMBL, all three NHCs promote no dimerization but polymerization, with the polymerization activity being highly sensitive to the NHC structure and the solvent polarity. Thus, I^{t}Bu is the most active catalyst of the series and converts quantitatively 1000−3000 equiv of MMBL in 1 min or 10 000 equiv in 5 min at room temperature to MMBL-based bioplastics with a narrow range of molecular weights of M_n = 70−85 kg/mol, regardless of the [MMBL]/[I^{t}Bu] ratio employed. The I^{t}Bu-catalyzed MMBL polymerization reaches an exceptionally high turnover frequency up to 122 s^{-1} and a high initiator efficiency value up to 1600%. Unique chain-termination mechanisms have been revealed, accounting for the production of relative high-molecular-weight linear polymers and the catalytic nature of this NHC-mediated conjugate-addition polymerization. Computational studies have provided mechanistic insights into reactivity and selectivity between two competing pathways for each NHC-monomer zwitterionic adduct, namely enamine formation/dimerization through proton transfer vs polymerization through conjugate addition, and mapped out extensive energy profiles for chain initiation, propagation, and termination steps, thereby satisfactorily explaining the experimental observations.

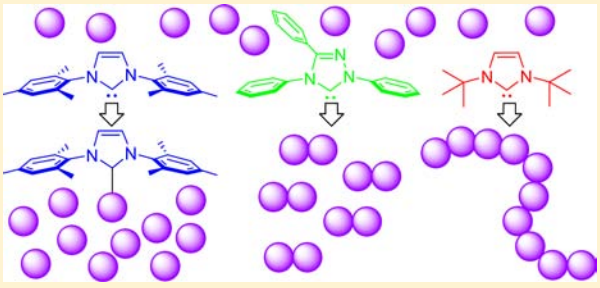

INTRODUCTION

Organocatalysis[1] using small-molecule organic compounds as catalysts has risen to prominence over the past decade in organic synthesis, polymer synthesis, and other areas, thanks to several advantages it can offer relative to other modes of catalysis. First, many small-molecule organic catalysts are commercially available, inexpensive, and air/moisture stable. Second, small-molecule organocatalysts are readily available from renewable resources and relatively nontoxic and thus "greener" than other types of catalysts. Third, asymmetric catalysis can be achieved by chiral organic reagents, many of which are naturally available from biological sources as single enantiomers. Overall, organocatalysis is especially advantageous when metal-free products or processes are of primary concern.

As an important class of organic catalysts, N-heterocyclic carbenes (NHCs) have attracted increasing interest due to their unique reactivity and selectivity observed in many different types of organic reactions.[2] Thanks to the pioneering work of Hedrick, Waymouth, and their co-workers,[3] the utility of the NHC-mediated reactions has been expanded to polymer synthesis,[4] via predominantly the ring-opening polymerization (ROP) of heterocyclic monomers, such as lactides,[5] lactones,[6] epoxides,[7] cyclic carbonates,[8] cyclic siloxanes,[9] and *N*-carboxyl-anhydrides.[10] NHC-mediated step-growth polymerization has been reported as well.[11] Polymerization of α,β-unsaturated esters (or acrylic monomers) such as methyl methacrylate

Received: September 3, 2013
Published: November 18, 2013

dx.doi.org/10.1021/ja4088677 | J. Am. Chem. Soc. 2013, 135, 17925−17942

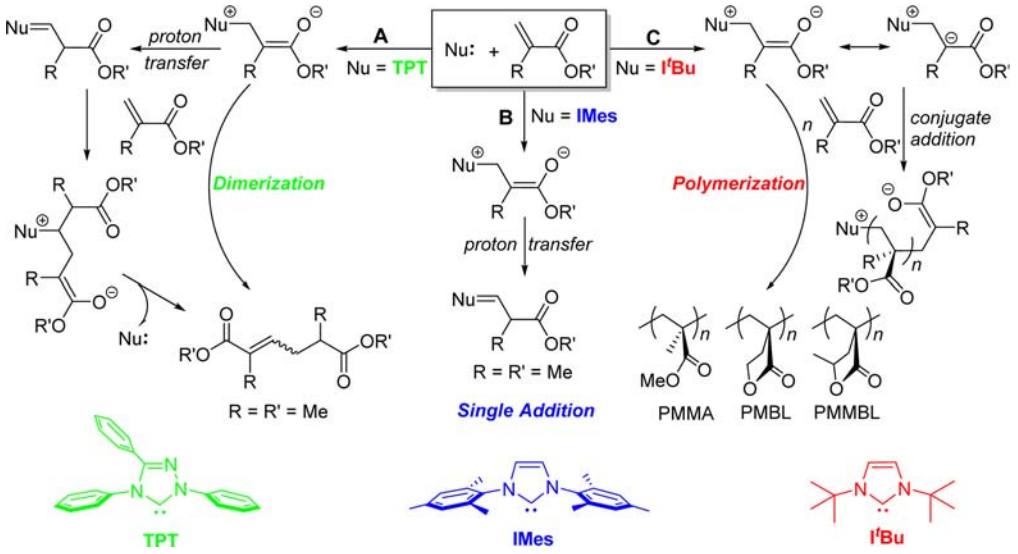

Figure 1. Outlined three distinctive reaction pathways involved in the reaction of NHCs and acrylic monomers.

(MMA) has also been recently realized through the classic group-transfer polymerization (GTP) initiated by a silyl ketene acetal (SKA),[12] using NHCs as alternative nucleophilic catalysts to the commonly used fluoride and oxygenated anionic catalysts for activating the SKA initiator.[13] In addition, such acrylic monomers can be rapidly polymerized by frustrated Lewis pairs (FLPs)[14] consisting of bulky NHC bases, such as the Arduengo carbenes 1,3-di-*tert*-butylimidazolin-2-ylidene (I^tBu) and 1,3-dimesitylimidazolin-2-ylidene (IMes),[15] and the strongly acidic, sterically encumbered pentafluorophenyl alane $Al(C_6F_5)_3$, via the proposed zwitterionic imidazolium enolaluminate intermediates.[16] Using such Arduengo NHCs alone, no MMA conversion was observed in either toluene[16] or THF.[13c] On the other hand, Glorius and Matsuoka discovered that the Enders triazolylidene carbene TPT (1,3,4-triphenyl-4,5-dihydro-1*H*-1,2,4-triazol-5-ylidene),[17] which was estimated to be 10^3 times less nucleophilic than the imidazolylidene carbene (IMes),[18] catalyzes tail-to-tail dimerization (umpolung) of MMA and other methacrylate substrates, while the common imidazolylidene carbenes are ineffective.[19]

It is clear from the above overview, although the NHC-mediated ROP of heterocyclic monomers has been highly successful, the NHC-mediated conjugate-addition polymerization of conjugated polar alkenes, such as acrylic monomers, still required the use of a nucleophilic initiator (SKA) in the case of GTP[13] or a Lewis acid catalyst [$Al(C_6F_5)_3$] in the case of the FLP polymerization.[16] When used alone (i.e., without combining with either the SKA initiator or the alane catalyst), NHCs such as I^tBu and IMes in toluene[16c] or (1,3-di-isopropyl-4,5-dimethylimidazolin-2-ylidene (I^iPrMe_2) in THF[13c] effected no monomer conversion in the MMA polymerization at ambient temperature, although the polymerization of *tert*-butyl acrylate by I^iPrMe_2 achieved 25% monomer conversion after 16 h.[13c] We[20] recently discovered that an NHC *alone* initiates extremely rapid conjugate-addition polymerization of cyclic acrylic monomers—renewable methylene butyrolactones,[21] including the naturally occurring α-methylene-γ-butyrolactone (MBL)[22] and the biomass-derived γ-methyl-α-methylene-γ-butyrolactone (MMBL).[23] The polymerization achieves quantitative monomer conversion in 1 min with a low I^tBu loading at room temperature (RT), affording medium- or high-molecular-weight (MW) polymers. The rate of the polymerization is strongly affected by the relative nucleophilicity of the NHC catalyst employed, with the most nucleophilic I^tBu in the series exhibiting the highest activity, the less nucleophilic IMes displaying a much lower activity, and the least nucleophilic TPT often showing no activity (in DMF) at all. Intriguingly, there exists a remarkable selectivity of the NHC for the substrate structure, thus leading to three different modes of reaction involving acrylic substrates (Figure 1):[20] TPT promotes dimerization of methacrylates such as MMA (pathway A); IMes selectively forms the single-addition product—the enamine or the deoxy-Breslow intermediate[19,20,24,25]—with methacrylates such as MMA (pathway B); and I^tBu mediates rapid polymerization of methylene butyrolactones such as MMBL (pathway C). That preliminary study generated many fascinating results on the NHC-mediated polymerization of acrylic monomers, but at the same time it brought forth four unaddressed important, fundamental questions: (a) What are the underlying reasons for the observed exquisite selectivity of the NHC structure for the three types of reactions it promotes: enamine formation, dimerization, and polymerization? (b) What are the mechanisms of chain initiation, propagation, and termination or transfer? (c) Is it a catalytic polymerization in the absence or presence of a suitable chain-transfer agent (CTA)? And (d) what is the structure of the resulting polymer, linear or cyclic? Accordingly, the central objective of this study was to address these important questions through combined experimental and theoretical/computational investigations, the results of which are presented herein.

RESULTS

Reactivity of NHCs toward MMA and MMBL. For MMA polymerization, NHCs such as I^tBu and IMes in toluene[16c] or I^iPrMe_2 in THF[13c] effected no monomer conversion at ambient temperature. However, depending on the NHC structure and the reaction medium, three types of interesting reactivity have been observed. Specifically, TPT exhibits no or negligible activity for polymerization of MMA in toluene or DMF, at RT or 80 °C, up to 24 h.[20] However, it catalyzes efficient tail-to-tail dimerization of MMA in toluene or polar solvents (e.g., DME or 1,4-dioxane) at 80 °C, affording dimethyl-2,5-dimethylhex-2-enedioate (E/Z = 95/5) in good yields (cf., pathway **A**, Figure

dx.doi.org/10.1021/ja4088677 | J. Am. Chem. Soc. 2013, 135, 17925−17942

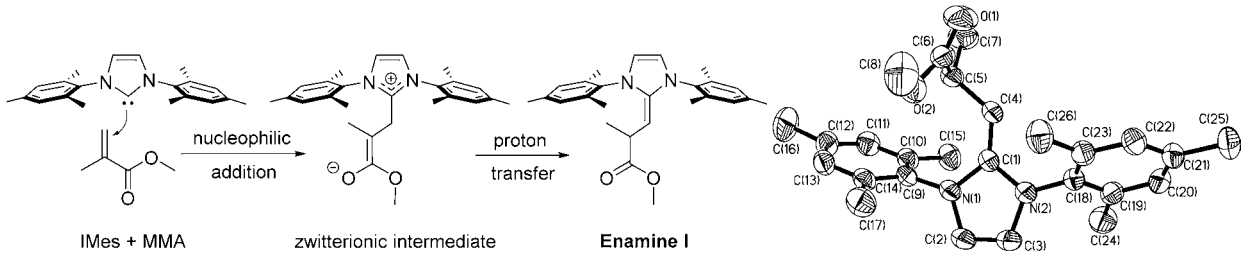

Figure 2. Formation of single-addition product enamine **I** (the deoxy-Breslow intermediate) from the reaction of MMA + IMes and its X-ray crystal structure. Hydrogen atoms were omitted for clarity and ellipsoids drawn at 50% probability. Selected bond lengths [Å]: C1−C4 = 1.353(2), C2−C3 = 1.316(2), C4−C5 = 1.508(2).

Table 1. Selected MMBL Polymerization Results by I^tBu in DMF at 25 °C[a]

run no.	[I^tBu] (mmol/L)	$[MMBL]_0/[I^tBu]_0$	time (s)	conv.[b] (%)	M_n[c] (kg/mol)	PDI[c] (M_w/M_n)	I^*[d] (%)
1	4.68	200	60	100	38.5	1.68	58.1
2	2.34	400	60	100	69.0	1.93	64.9
3	1.17	800	60	100	84.7	2.11	106
4	0.936	1000	60	>99	71.9	1.80	154
5	0.312	3000	60	>99	88.7	1.45	375
6	0.187	5000	120	>99	81.2	1.48	683
7	0.117	8000	15	33.4	52.6	2.10	569
8			30	58.3	67.1	2.00	778
9			45	69.6	72.9	2.00	855
10			60	81.8	76.3	1.99	961
11			80	88.6	78.1	1.97	1016
12			100	93.5	77.7	1.98	1078
13			120	95.5	79.0	1.97	1083
14			150	97.2	78.8	1.97	1105
15			180	99.0	79.9	1.93	1110
16	0.0936	10 000	20	18.3	44.3	1.98	463
17			40	55.2	64.6	2.03	957
18			60	69.4	73.4	1.96	1059
19			80	78.2	76.8	1.96	1140
20			100	81.7	79.5	1.92	1151
21			120	86.3	78.8	1.94	1226
22			180	94.6	81.0	1.92	1308
23			250	97.3	78.6	1.98	1386
24			300	98.5	79.3	1.96	1391
25	0.0780	12 000	20	19.5	45.9	2.33	571
26			40	30.8	53.1	2.07	780
27			60	33.8	53.5	1.98	849
28			80	36.0	55.7	2.00	869
39			100	47.2	59.8	2.05	1061
30			120	50.1	64.0	1.97	1052
31			150	56.8	65.7	2.00	1162
32			180	61.5	69.1	2.00	1196
33			210	68.9	69.3	2.01	1336
34			240	71.1	71.3	1.96	1340
35			300	75.1	70.9	1.99	1424
36			360	79.3	74.1	1.95	1438
37			420	81.5	72.6	1.96	1509
38			600	85.3	72.9	1.96	1573
39			900	88.3	74.2	1.95	1599

[a]Carried out at ambient temperature (~25 °C) in 4.5 mL DMF and 0.5 mL MMBL solution with fixed $[MMBL]_0$ = 0.936 M. [b]Monomer conversions measured by ^1H NMR. [c]M_n and PDI determined by gel-permeation chromatography (GPC) in DMF relative to PMMA standards. A small (0.1−2%) high-molecular-weight peak (>10^6 g/mol), attributable to the polymer aggregation, was present in most of the samples. [d]Initiator efficiency (I^*) = M_n (calcd)/M_n (exptl), where M_n (calcd) = MW(M) × [M]/[I] × conversion (%) + MW (chain-end groups).

1), while the common imidazolylidene carbenes are ineffective.[19] This intermolecular umpolung of MMA was proposed to proceed through the initial conjugate addition of TPT to MMA to form the corresponding ester enolate that undergoes proton transfer (or tautomerization) affording an enamine intermediate, the deoxy-Breslow intermediate analogous to the Breslow

dx.doi.org/10.1021/ja4088677 | J. Am. Chem. Soc. 2013, 135, 17925−17942

intermediate involved in the benzoin reaction;[26] addition of the enamine to another molecule of MMA leads to the tail-to-tail dimerization product, via again the ester enolate intermediate that undergoes proton transfer and release of TPT.[19] This mechanism bears a close resemblance to the one proposed for the intramolecular umpolung of Michael acceptors catalyzed by NHCs.[27] We found that, despite the fact that I^{t}Bu did not react with MMA in toluene at RT (up to 3 days), IMes reacted smoothly with MMA at RT to form a single-addition product, enamine, or deoxy-Breslow intermediate **I** (Figure 2). Unlike the TPT-derived enamine intermediate involved in the dimerization of MMA, the enamine derived from IMes is stable, isolable, and nonreactive toward additional MMA, presumably due to its strong, irreversible binding of IMes with MMA and high-energy barrier for conjugate addition to another MMA molecule (cf., pathway **B**, Figure 1). Noteworthy is that the reaction of TPT and MMA at RT also forms the enamine as two isomers (enamine **II**, see the Supporting Information for details); but unlike the IMes-based enamine **I**, upon heating to 80 °C enamine **II** further reacts with MMA to form the dimer in a catalytic fashion. The molecular structure of enamine **I** (Figure 2) clearly displays a C=C double bond formed between C1 and C4 carbons, with a bond distance of 1.353(2) Å. This single-addition product resembles those enamines derived from the 1:1 addition of TPT to more highly (doubly) activated Michael acceptors.[17,28] Although the structurally characterized aza-Breslow intermediate[29] and the methylated enaminol Breslow intermediate[30] have been reported previously, enamine **I**[20] and other analogous intermediates derived from NHC[31] represent the structurally characterized deoxy-Breslow intermediate.

Intriguingly, although I^{t}Bu exhibits no reactivity toward MMA in toluene or THF (neither enamine formation nor dimerization) and neither TPT nor IMes polymerizes MMA at RT, 0 °C, or −40 °C in toluene or DMF, I^{t}Bu polymerizes MMA in DMF at RT with an appreciable activity. With a 0.5 mol % loading of I^{t}Bu, the MMA polymerization in DMF (8.0 mL) at RT achieved 68% conversion in 1 h, corresponding to a good turnover frequency (TOF) of 136 h^{-1}. The PMMA produced is a syndio-rich atactic material, with syndiotacticity (*rr*) = 55.7%, heterotacticity (*mr*) = 39.6%, and isotacticity (*mm*) = 4.7%, typical tacticity values of PMMA produced by anionic polymerization in polar donor solvents at RT.[32] The number-average molecular weight (M_n) of the PMMA was 33.2 kg/mol (at 87% monomer conversion), with a polydispersity index (PDI) of M_w/M_n = 1.99. As this measured M_n was much higher than the calculated M_n (17.4 kg/mol) according to the $[MMA]_0/[I^tBu]_0$ ratio employed, the resulting initiator efficiency (I^* = M_n (calcd)/M_n (exptl), where M_n (calcd) = MW(M) × [M]/[I] × conversion (%) + MW (chain-end groups)) was only 52%. We also carried out a series of MMA polymerizations at RT with a fixed monomer concentration of $[MMA]_o$ = 0.936 (in 4.5 mL DMF) but varying the $[MMA]_0/[I^tBu]_0$ ratio from 200, 400, 800, to 1000, and found that the resulting initiator efficiencies for these runs, calculated on the basis of the measured monomer conversion and polymer M_n values, were in the range of 12−30%. Overall, these results indicate that the MMA polymerization by ^{t}Bu in DMF has a typical initiator efficiency value of only ∼50% or lower, thus a noncatalytic process.

The bioderived MMBL can be described as the cyclic analog of MMA; however, it exhibits greater reactivity in chain-growth polymerization than typical alkyl methacrylates such as MMA, attributable to the presence of both the nearly planar five-membered lactone ring (which provides resonance stabilization for the active species) and the higher energy exocyclic C=C double bond (as a result of the ring strain and the fixed *s-cis* conformation).[21] As a result, MMBL behaves rather differently toward NHCs than MMA. First, TPT (0.5 mol %) exhibited no activity toward MMBL in either THF or DMF at RT up to 24 h, but in toluene it showed some polymerization activity, achieving 79% monomer conversion in 24 h (TOF = 7 h^{-1}) and producing PMMBL with M_n = 38.9 kg/mol. Second, the more nucleophilic IMes is more active in MMBL polymerization; for instance, the MMBL polymerization by IMes (0.5 mol %) at RT achieved 98% and 100% monomer conversion after 24 h, affording PMMBL with M_n = 51.2 and 17.8 kg/mol, in toluene and DMF, respectively. IMes also polymerizes MMBL at 80 °C in toluene with no enamine formation. Third, the most nucleophilic NHC of the series, I^{t}Bu, is the most active catalyst. In toluene, the MMBL polymerization by I^{t}Bu (0.5 mol %) achieved 93% conversion in only 30 min, affording the relatively high-molecular-weight PMMBL (M_n = 58.4 kg/mol). Switching to DMF, the polymerization was complete in less than 1 min. In fact, quantitative monomer conversion was achieved in <1 min with a [MMBL]/[I^{t}Bu] ratio as high as 3000 (i.e., 0.03 mol % I^{t}Bu), giving rise to a very high TOF of >1.8 × 10^5 h^{-1} (51 s^{-1}).

Table 1 summarizes selected MMBL polymerization results by I^{t}Bu in DMF at RT with varied [MMBL]/[I^{t}Bu] ratios from 200 to 12 000. As in the polymerization of MMBL mediated by metal- and metalloid-based catalysts or initiators,[21a−h] no ring-opening of the butyrolactone ring was observed; control runs using NHCs or NHC/Lewis acid pairs for the ROP of five-membered lactones, γ-butyrolactone and γ-valerolactone, also showed no polymerization activity. Overall, these results established I^{t}Bu as the best and most active catalyst of the current NHC series for rapid polymerization of acrylic monomers, especially the biorenewable MMBL (cf., pathway **C**, Figure 1).

Characteristics and Kinetics of MMBL Polymerization by I^{t}Bu. Having established I^{t}Bu as the best catalyst system in all aspects for the MMBL polymerization in DMF, we subsequently examined this polymerization in more detail, specifically concerning its degree of control and kinetics that varied the [MMBL]/[I^{t}Bu] ratios from 200 to 15 000 (Table 1). As can be seen from this table, the MMBL polymerization by I^{t}Bu is exceedingly rapid, achieving quantitative monomer conversion in <1 min with the [MMBL]/[I^{t}Bu] ratio as high as 3000 (runs 1−5). At higher [MMBL]/[I^{t}Bu] ratios, the polymerization can still achieve quantitative or near quantitative monomer conversion at progressively longer reaction times: 5000 in 2 min (run 6), 8000 (99%) in 3 min (run 15), and 10 000 (99%) in 5 min (run 24). At an even higher [MMBL]/[I^{t}Bu] ratio of 12 000, the polymerization achieved 88% conversion in 15 min (run 39). The TOF for the polymerization of MMBL by 0.01 mol % I^{t}Bu, calculated from the maximum slope of the conversion vs time plot (Figure 3), was high, 4.4 × 10^5 h^{-1} (122 s^{-1}). This high rate of polymerization is compared to a k_{app} of 26.5 s^{-1} for the MMA polymerization by anionic polymerization using tetrakis[tris(dimethylamino)-phosphoranylidenamino]phosphonium (P_5^+) as the counterion in THF[33] and to a TOF value of 26 h^{-1} for a typical anionic polymerization of MMBL by BuLi in THF ([MMBL]/[BuLi] = 60, 2 h, 86% conversion).[34]

dx.doi.org/10.1021/ja4088677 | J. Am. Chem. Soc. 2013, 135, 17925−17942

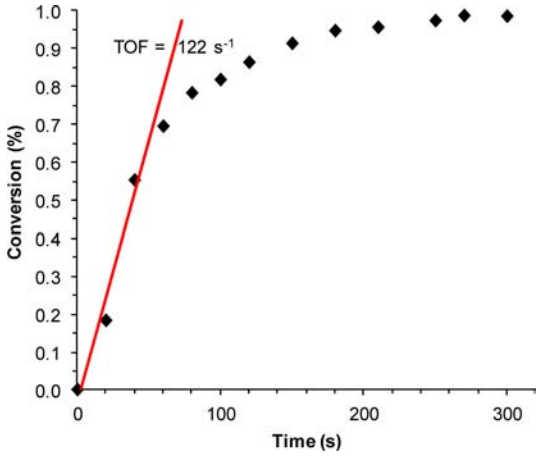

Figure 3. MMBL conversion (%) vs time (s) plot. Conditions: [MMBL]/[I^{t}Bu] = 10 000, DMF, 25 °C.

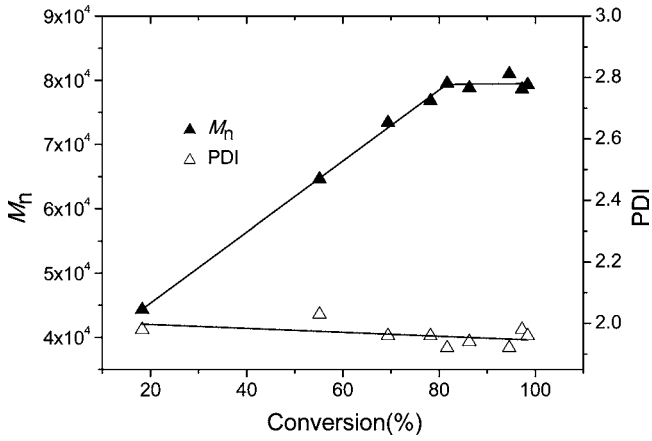

Figure 4. Plots of M_n and PDI of PMMBL vs MMBL conversion in DMF at 25 °C: $[MMBL]_0$ = 0.935 M, $[I^tBu]$ = 0.0936 mM with a $[MMBL]_0/[I^tBu]_0$ ratio of 10 000/1.

Another interesting feature of this polymerization, observed through analysis of the resulting polymer molecular weights vs the calculated values, is large variations of the initiator efficiency I^* as a function of the [MMBL]/[I^{t}Bu] ratio. When this ratio was ≤400, the calculated I^* was lower than 100% (58−65%), suggesting a slower rate of initiation relative to the rate of propagation and/or decomposition of the initiator or the active species. An experiment was then designed to determine which scenario is applicable to the present system. Specifically, a small scale MMBL polymerization by I^{t}Bu was carried out in toluene-d_8. The resulting polymer was removed by filtration after all the monomer had been converted, and the filtrate was analyzed by ^{1}H NMR. Most of I^{t}Bu still remained in the filtrate, implying that only a small amount of I^{t}Bu was involved in the initiation step (which is still attached to the polymer chain) due to the lower initiation rate, relative to the rate of propagation. When the [MMBL]/[I^{t}Bu] ratio was 800, the measured M_n of 84.7 kg/mol matched almost perfectly with the calculated M_n, thus affording a near quantitative I^* value of 106% (run 3). A further increase in the [MMBL]/[I^{t}Bu] ratio to 1000, 3000, and 5000 resulted in a steady increase in the I^* value to 154% (run 4), 375% (run 5), and 683% (run 6), respectively. The I^* continued to go up to 1110% (run 15) in the 8000 ratio and 1391% (run 24) in the 10 000 ratio and reached the highest 1600% (run 39) in the 12 000 ratio. These results indicate substantial internal chain transfer occurred, even in the absence of any added suitable CTAs, thus producing multiple polymer chains (up to 16 chains) per initiator molecule, indicative of a catalytic polymerization system through chain transfer to monomer.

Figure 4 depicts the profile of M_n of PMMBL vs MMBL conversion in a high [MMBL]/[I^{t}Bu] ratio of 10 000. A linear increase of M_n with MMBL conversion was observed at early and mid stages of the polymerization up to 80% conversion. However, at later stages of polymerization the polymer MW remained nearly constant (79−81 kg/mol, runs 20−24, Table 1) with monomer conversion up to completion, indicative of chain termination or transfer (i.e., chain termination followed by chain reinitiation) effectively competing with chain propagation. The MW distribution corresponds to what is expected for chain growth with chain transfer, that is $M_w/M_n \approx 2.0$.[35] Comparing the M_n values of the final isolated polymers with different [MMBL]/[I^{t}Bu] ratios, we found the M_n increased with the increasing of the [MMBL]/[I^{t}Bu] ratio initially and then remained nearly constant when this ratio was higher than 800 (Figure 5). Possible physical reasons due to

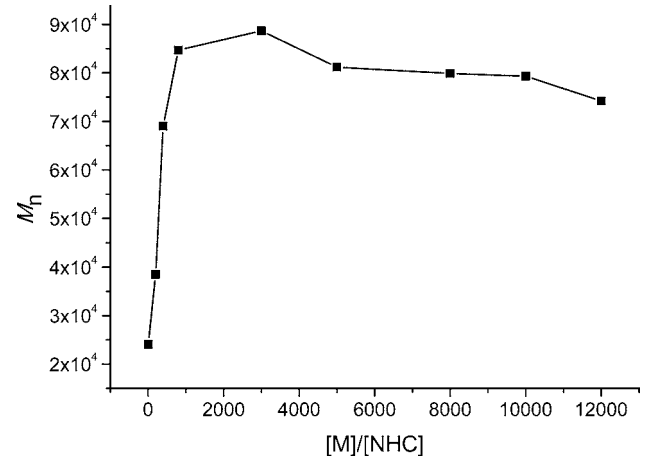

Figure 5. Plot of M_n of PMMBL vs [MMBL]/[I^{t}Bu] ratio.

viscosity/solubility issues are unlikely in this case as the polymer at this MW range is very soluble in DMF. Furthermore, carrying out the 1000:1 ratio polymerization in more dilute conditions (using 9.5 mL DMF) produced PMMBL with M_n = 67.8 kDa (PDI = 1.96), which is rather similar to that produced under current standard conditions (4.5 mL DMF). However, switching the solvent to toluene enabled the polymerization to produce PMMBL with a much higher MW of M_n = 107 kDa (PDI = 2.99) at 93% conversion after 4 h; the polymerization was much slower, and the resulting polymer crashed out of the solution, but this much higher MW yielded a nearly quantitative initiator efficiency of I^* = 97% (thus no chain transfer). The above observations, together with the high I^* values, demonstrate that this polymerization in DMF is an effective catalytic polymerization system through internal chain transfer when the [MMBL]/[I^{t}Bu] ratio is higher than 800. This scenario can be examined by sequential addition of monomer. Specifically, two chain-extension polymerizations with a [MMBL]/[I^{t}Bu] ratio of 1000 were carried out to verify the catalytic property of the polymerization. Upon complete conversion of the initial monomer pool, an additional 1000 and 500 equiv of the monomer was added to a total monomer

dx.doi.org/10.1021/ja4088677 | J. Am. Chem. Soc. 2013, 135, 17925−17942

concentration of 1.87 and 1.40 M, respectively. The reaction was allowed to completion. GPC analysis of the resulting polymers showed that both final polymers exhibited unimodal MW distribution, and the M_n of the polymers were identical (Figure 6), even though the total combined [MMBL]/[I^{t}Bu] ratios were different (i.e., 2000 vs 1500).

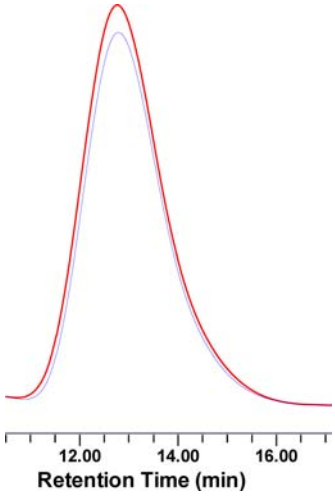

Figure 6. Overlay GPC traces of the two sequential polymerizations with a different combined [MMBL]/[I^{t}Bu] ratio of 2000 (red) and 1500 (blue).

Kinetic experiments employed the $[MMBL]_0/[I^tBu]_0$ ratios ranging from 5000 to 15 000 (i.e., with 0.02−0.0067 mol % I^{t}Bu loadings). Even with such low catalyst loadings, a considerable amount of monomer had already been converted into polymer by the first data point could be collected (e.g., 18.3% monomer conversion was observed in 20 s of the reaction with 0.02 mol % I^{t}Bu). Although the kinetic profile of the polymerization at the earlier stage of the reaction was not captured, the kinetic plots with the available data clearly showed a first-order dependence on monomer concentration for all the ratios investigated (Figure 7). Furthermore, a double logarithm plot (Figure 8) of the apparent rate constants (k_{app}), obtained from the slopes of the best-fit lines to the plots of $\ln([MMBL]_0/[MMBL]_t)$ vs time for the three [MMBL]/[I^{t}Bu] ratios of 5000

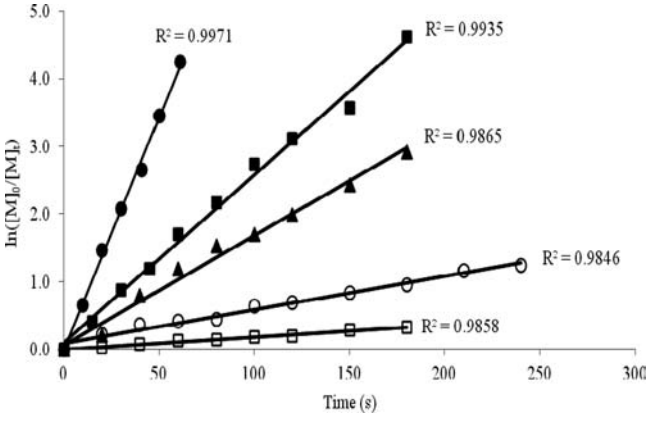

Figure 7. Plots of the first-order kinetics of $\ln([MMBL]_0/[MMBL]_t)$ vs time (sec) for the MMBL polymerization by I^{t}Bu in DMF at 25 °C. Conditions: $[MMBL]_0$ = 0.935 M; $[I^tBu]_0$ = 0.187 (●), 0.117 (■), 0.0936 (▲), 0.0780 (○), and 0.0624 (□) mM.

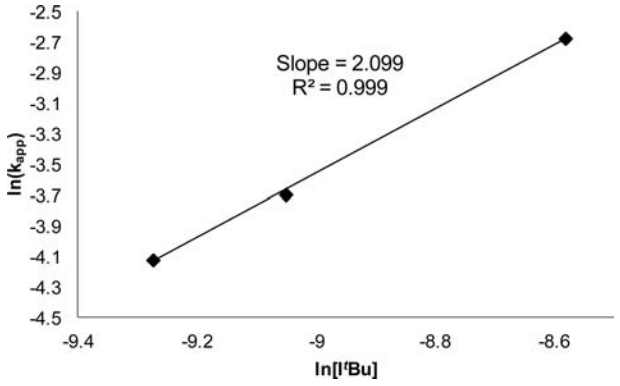

Figure 8. Plot of $\ln(k_{app})$ vs $\ln[I^tBu]$ for the MMBL polymerization by I^{t}Bu in DMF at 25 °C.

(0.02 mol % I^{t}Bu), 8000 (0.0125 mol % I^{t}Bu), and 10 000 (0.01 mol % I^{t}Bu), as a function of $\ln[I^tBu]_0$, was fit to a straight line (R^2 = 0.999) with a slope of 2.099. Thus, the kinetic order with respect to [I^{t}Bu], given by the slope of ∼2, reveals that the overall polymerization is second order in I^{t}Bu concentration. The mechanistic scenario revealed by our computational studies (vide infra) indicates the slowest step of the I^{t}Bu-mediated MMBL polymerization process is the formation of the I^{t}Bu-MMBL adduct (i.e., chain initiation to generate the zwitterionic active propagating specie), thus in agreement with the observed first-order dependence on monomer concentration. However, it is not obvious why there was a second-order dependence on [I^{t}Bu], but factors contributing to this experimental observation could include inefficient chain initiation or reinitiation by I^{t}Bu and, especially under such low catalyst loading conditions, catalyst decomposition and poisoning by the adventitious impurities brought into the system from the solvent and/or monomer.

Chain Termination and End Groups. A possible mechanistic scenario for the conjugate-addition polymerization of acrylic monomers by NHCs was proposed to proceed through reiterative 1,4-conjugate addition of the propagating ester enolate to the incoming monomer (cf., pathway C, Figure 1),[20] following the well-established conjugate-addition mechanism for the controlled anionic polymerization of acrylics using discrete or in situ generated metal ester enolates.[32] Determination of the polymer chain structure, including chain-end groups, typically provides critical insight into chain termination and/or transfer mechanisms. To this end, analysis of low-molecular-weight MMBL oligomers produced with NHCs (TPT or I^{t}Bu) in toluene by MALDI-TOF MS showed that neither initiating nor terminating end-groups were present in the major fraction of the oligomers (Figure 9 by TPT; Figure S7 by I^{t}Bu); this result may indicate a possible cyclic chain structure due to the absence of any end groups seen by the MS method, and the fact that it is known that the NHC-initiated zwitterionic ROP of lactide produces cyclic poly(lactide).[4,5] The origin of such structure for the current conjugate-addition polymers could be explained by a mode of chain termination via backbiting of the growing ester enolate to the electrophilic carbon directly bonded to the NHC, accompanied by elimination of the NHC (Scheme 1).

Two alternative hypotheses based on the linear polymer structure could also explain the MALDI-TOF MS result. The first structure could be formed through a sequence of events involving abstraction of a proton α to the NHC by the enolate

dx.doi.org/10.1021/ja4088677 | J. Am. Chem. Soc. 2013, 135, 17925−17942

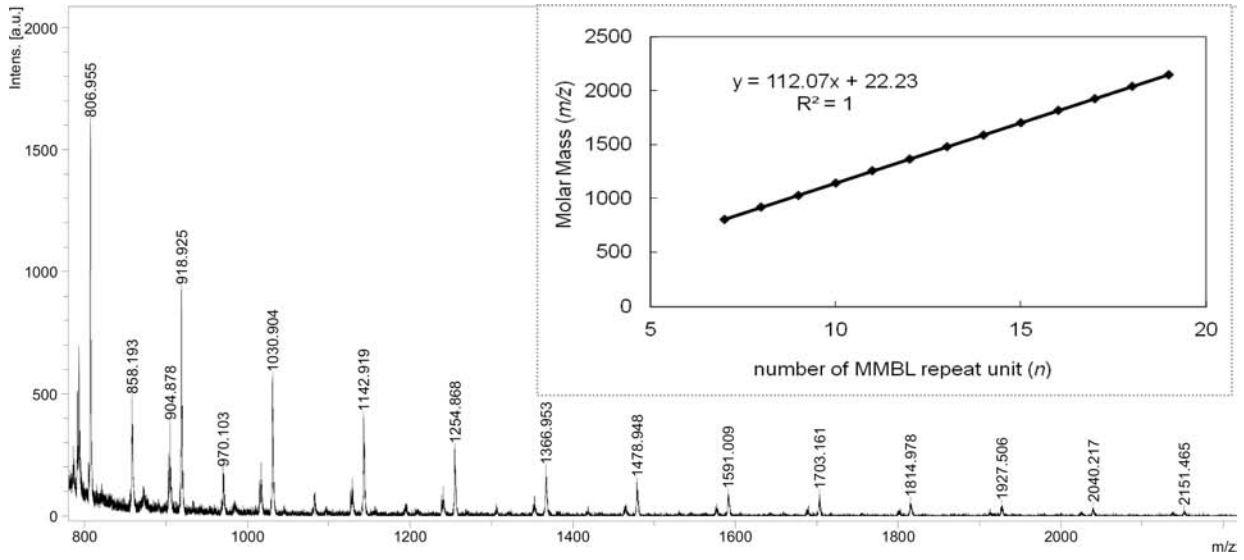

Figure 9. MALDI-TOF MS spectrum of low-molecular-weight MMBL oligomers produced by TPT in toluene at RT. Inset: plot of m/z values of the major mass series vs the number of MMBL repeat units (n). The slope of 112.07 corresponds to the mass of the MMBL repeat unit and the intercept of 22.23 is a sum of the masses of Na^+ (from the added NaI) and end groups (none).

Scheme 1. Possible Pathways Leading to Cyclic and Linear Polymers

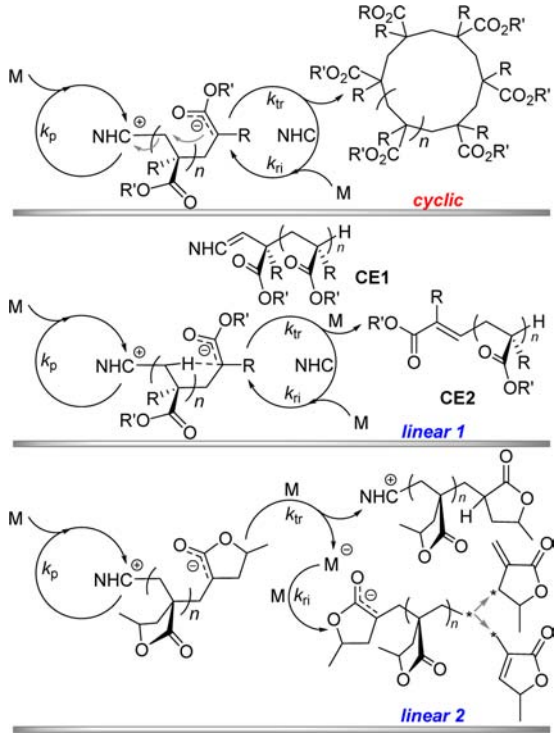

chain end to form an enamine intermediate, **CE1**, which reacts with another monomer to form a linear polymer with chain end structure **CE2** (Scheme 1), accompanied by release of the NHC (cf., Discussion, vide infra). The released NHC initiates a new chain, thereby effecting a catalytic polymerization. The last step of the reaction sequence, **CE1** + M → **CE2** + NHC, is analogous to the NHC-catalyzed tail-to-tail dimerization (umpolung) of methacrylates.[19] In the chain end structure of **CE2**, one MMBL unit on one chain end loses an H atom, while the other MMBL unit on the other chain end gains an H atom and, overall, as if the whole chain had no end groups seen by MALDI-TOF MS. The second structure, in the case of MMBL polymerization, could be formed through abstraction of an H from the β-C of the monomer by the reactive enolate chain end to generate the saturated chain with the cation $[NHC]^+$ still attached to it and the monomer anion that reinitiates a new chain, also effecting a catalytic polymerization (Scheme 1).

To provide experimental evidence to distinguish these two possible chain structures (cyclic vs linear), we utilized GPC with a light scattering detector coupled to a viscometer to analyze and compare the PMMBL samples of similar MW prepared with I^tBu and the GTP method initiated by a SKA, $Me_2C{=}C(OMe)OSiMe_3$, the latter method of which is known to produce linear MMBL polymers.[21a,f] A Mark–Houwink plot of the two types of the PMMBL samples is depicted in Figure 10, featuring indistinguishable intrinsic viscosities of the polymers; in essence, if the PMMBL produced by I^tBu had a cyclic structure, then one would observe lower intrinsic viscosity for the cyclic polymer than the linear one, with a $[\eta]_{cyclic}/[\eta]_{linear}$ ratio of ~0.7.[36] The two classes of polymers also showed nearly superimposable linearly fit plots of $\log(M_w)$ vs elution volume for the same hydrodynamic volumes. Overall,

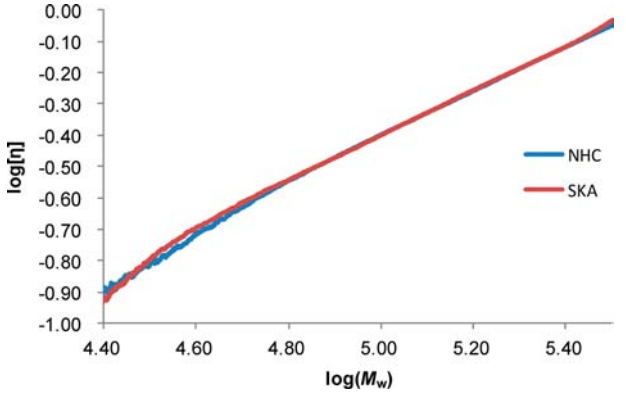

Figure 10. Double logarithm plot of intrinsic viscosity $[\eta]$ vs weight-average molecular weight (M_w) for PMMBL by NHC and SKA initiators.

dx.doi.org/10.1021/ja4088677 | J. Am. Chem. Soc. 2013, 135, 17925–17942

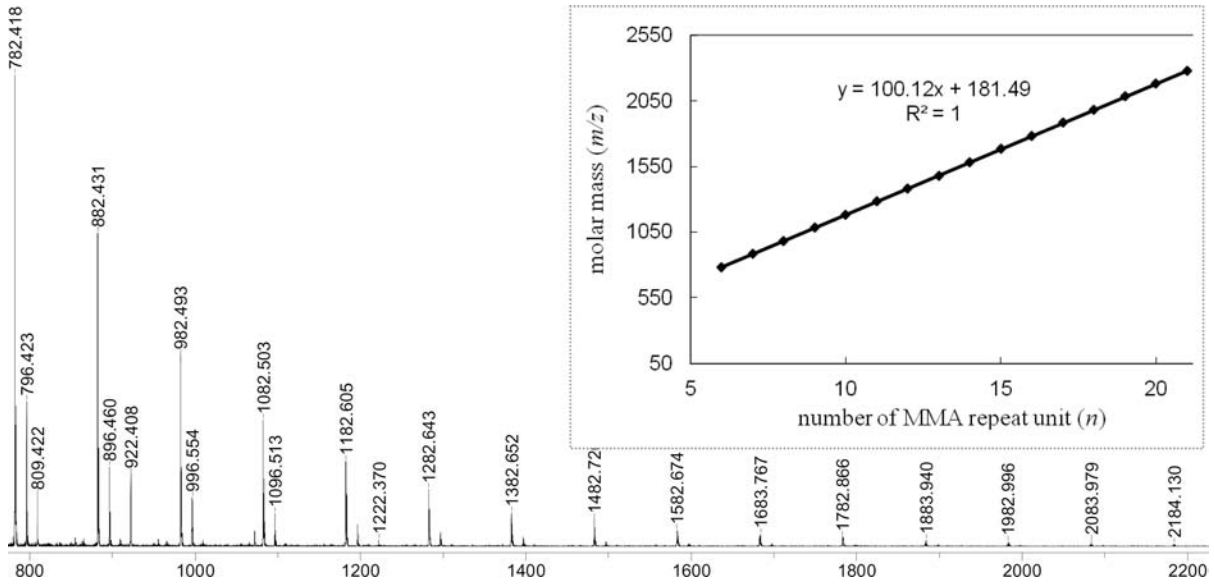

Figure 11. MALDI-TOF MS spectrum of low-molecular-weight MMA oligomers produced by I^{t}Bu in DMF at RT. Inset: plot of m/z values of the major mass series vs the number of MMA repeat units (n).

these results clearly indicate the PMMBL produced by I^{t}Bu has a linear structure.

To identify the termination chain-end groups of the linear polymer, two low-molecular-weight PMMBL samples produced by I^{t}Bu were characterized by ^{1}H NMR. One of them was produced by I^{t}Bu in a low $[MMBL]_0/[I^tBu]_0$ ratio of 5:1 in DMF at −40 °C. The solvent was removed, and the product was washed by hexanes. The ^{1}H NMR (Figure S8) exhibits peaks at δ 7.10 ppm (d, 1H, J = 3.2 Hz, N−C*H*=CH−N) and 6.46 ppm (d, 1H, J = 3.6 Hz, N−CH=C*H*−N), characteristics of the protons on the imidazole ring of the enamine intermediate, specifically chain end structure type **CE1** (Scheme 1). The other low-molecular-weight PMMBL was produced by I^{t}Bu in toluene at RT. The ^{1}H NMR (Figure S8) exhibits peaks at δ 6.44 ppm (br, 1H, −C*H*=), 6.36 ppm (br, 1H, −C*H*=), 4.46 ppm (br, 1H, OC*H*Me), and 2.61 ppm (br, 2H, CH_2CH=), consistent with chain end structure type **CE2** (Scheme 1). On the other hand, for the polymers produced at high [MMBL]/[I^{t}Bu] ratios (e.g., 10 000 or 12 000) in DMF at RT, several small peaks in the olefinic region were observed at 6.21, 5.60, and 6.70 ppm, attributable to the protons of the exocyclic double bond (6.21 and 5.60, which are similar, but not identical, to those the MMBL monomer peaks at 6.14 and 5.58 ppm), and the internal double bond (6.70 ppm), respectively, as a result of chain transfer to monomer and reinitiation processes (Scheme 1). Overall, the above combined studies by MALDI-TOF MS, GPC, NMR, and computational methods (vide infra) concluded the PMMBL produced by NHCs at RT is a linear polymer with different chain end groups, depending on polymerization conditions. The origin of such end groups and the accompanying chain termination and transfer mechanisms are described in the Discussion section.

Interestingly for MMA polymerization by I^{t}Bu in DMF at RT, the resulting PMMA had different chain end characteristics than those of PMMBL. Figure 11 depicts the MALDI-TOF MS of low-molecular-weight MMA oligomers and the plot of m/z values vs the number of MMA repeat units (n), the latter of which yielded a straight line with a slope of 100.1 and an intercept of 181.4. The slope corresponds to the mass of the MMA monomer, whereas the intercept is the sum of the masses of the chain-end groups corresponding to the I^{t}Bu moiety. Corroborating with this result, the ^{1}H NMR exhibited similar peaks to those depicted in Figure S8 for the enamine intermediate, namely chain end structure **CE1**. Hence, in the case of MMA polymerization by I^{t}Bu, the chain end generated is **CE1**, not **CE2**. In other words, the chain termination stops at **CE1**; hence, the MMA polymerization by I^{t}Bu appears to be noncatalytic as the NHC or other nucleophiles are not regenerated for chain reinitiation during the chain termination step.

Chain Transfer and Effects of Chain Transfer Agents. We hypothesized that catalytic polymerization of acrylics by NHCs can be achieved by an internal or external chain-transfer pathway outlined in Scheme 2. As described above, the internal chain transfer relies on either a chain-termination process that liberates NHC to reinitiate multiple chains or a chain transfer to monomer that generates the monomer anion to reinitiate multiple chains; the former process would be effective at later stages of a polymerization reaction, while the latter process would be favored at a high [monomer] to [NHC] ratio (vide supra). The external chain transfer could proceed in the presence of suitable CTAs such as enolizable organic acids which terminate the growing ester enolate chain via protonation, followed by nucleophilic attack of the resulting enolate anion to the electrophilic carbon directly bonded to Nu, releasing the catalyst (Scheme 2). Alternatively, the resulting enolate can directly initiate new chains.

Scheme 2. Proposed Chain Transfer Pathway via Addition of an External CTA

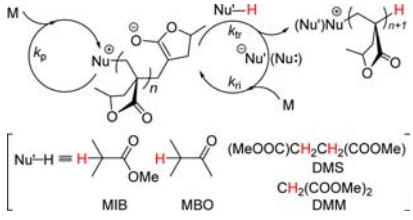

To achieve effective external chain transfer, we examined four organic acids, methyl isobutyrate (MIB), 3-methyl butanone (MBO), dimethyl succinate (DMS), and dimethyl malonate (DMM), with a decreasing order of their pK_a's (DMSO) values: MIB (~29) > MBO (~27) ≈ DMS ≫ DMM (15.9). In comparison, the conjugate acid pK_a (DMSO) of I^{t}Bu was reported to be ~23 (23.2[37] or 22.7[38]). Based on these pK_a values, we reasoned that the acidity of MIB will be too low to protonate the growing ester enolate chain end and thus not be an effective CTA, but MBO and DMS should be effective CTAs as their acidity is higher than the ester, the resulting product of protonation of the growing ester enolate chain. Moreover, DMM should be able to protonate I^{t}Bu and generate the corresponding imidazolium carbanion ion pair. The relative acidity of different CTAs vs I^{t}Bu can be confirmed by their reactions with I^{t}Bu in toluene-d_8. Thus, the ^{1}H NMR showed that no reaction occurred between I^{t}Bu and MIB, MBO, or DMS. However, a white precipitate was formed immediately upon mixing DMM with I^{t}Bu. The NMR (CD_2Cl_2) of the solid collected by filtration showed the formation of the corresponding ion pair $[I^tBuH]^+[CH(COOMe)_2]^-$ (as two isomers). The structure of this ion pair (*E* isomer) was further confirmed by X-ray diffraction analysis (Figure 12).

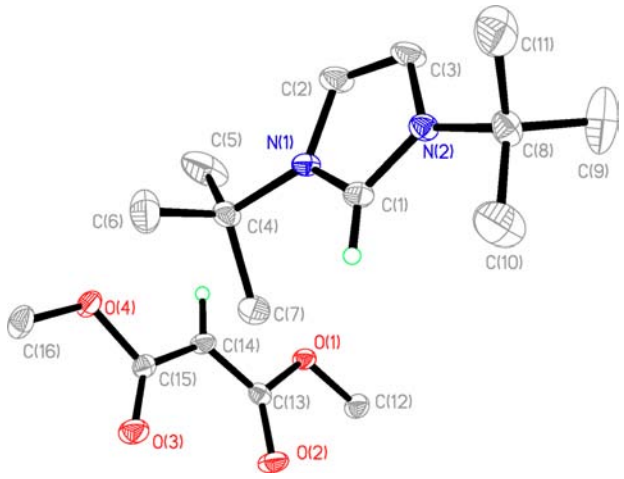

Figure 12. X-ray crystal structure of $[I^tBuH]^+[CH(COOMe)_2]^-$ (*E* isomer) with thermal ellipsoids drawn at the 50% probability.

Indeed, MIB was showed to be ineffective as a CTA because the M_n of the resulting PMMBL was not significantly affected by varying the amount of MIB (from 1 to 100 equiv relative to I^{t}Bu, runs 2−6 vs run 1, Table 2). On the other hand, a gradual increase in the amount of MBO added from 1 to 100 equiv relative to I^{t}Bu resulted in a corresponding decrease in M_n 68.3−29.2 kg/mol (runs 7−11); a further increase in the MBO added to 1000 equiv lowered the M_n to only 15.4 kg/mol (run 12). Moreover, addition of MBO did not noticeably affect the polymerization rate, achieving quantitative monomer conversion in 1 min for all runs), which implies that the relative rate constants for propagation (k_p) and reinitiation (k_{ri}) by the resulting ketone enolate are about the same ($k_p \approx k_{ri}$); thus, this chain-transfer polymerization with observed decrease in M_n while maintaining the more or less same polymerization rate upon addition of the CTA can be characterized as a "normal chain-transfer" polymerization.[39] As the chain initiation by the NHC nucleophile is slow relative to propagation, the above results suggest the chain reinitiation is predominately by the ketone enolate nucleophile Nu′, rather than by the NHC Nu (cf., Scheme 2).

The behavior of DMS as a CTA was similar to MBO (runs 13, 14 vs 8, 12), due to their similar acidity. In sharp contrast, the MMBL polymerization with DMM as a CTA showed a drastic decrease in the polymerization rate as the amount of DMM added increased (runs 15−21). This observation is indicative of ineffective reinitiation (i.e., $k_{ri} < k_p$), which is due to the fact that the nucleophilicity of the enolate $[CH(COOMe)_2]^-$ derived from DMM is much lower than that of the growing ester enolate. Nevertheless, DMM is the most efficient CTA of the series in terms of the ability to control the polymer MW. This conclusion was drawn by comparing chain-transfer constants (C_{tr}), defined as the ratio of rate constants of chain transfer to propagation, $C_{tr} = k_{tr}/k_p$.[39] Specifically, C_{tr} values were obtained from the slopes of linear plots of $1/M_n$ vs the [CTA]/[M] ratio (Figure 13). Accordingly, C_{tr} ($\times 10^4$) values for the MMBL polymerization by I^{t}Bu with MBO and DMM as CTAs were estimated to be 1.99 and 30.1, respectively. To confirm that the reinitiation is predominately through the enolate as a result of the chain transfer rather than by the NHC, low-molecular-weight MMBL oligomers produced by I^{t}Bu with DMM as the CTA were analyzed by MALDI-TOF MS (Figure 14). A plot of m/z values of the major mass series vs the number of MMBL repeat units (n) yielded a straight line with a slope of 112.06 and an intercept of 154.95. The slope corresponds to the mass of the MMBL monomer, whereas the intercept is the sum of the masses of the masses of Na^+ (from the added NaI, 23) and end groups (DMM, 132). This result clearly shows that a large majority of the chains were produced by the CTA-based enolate.

We also examined the behavior of catalytic chain-transfer polymerization of the parent methylene butyrolactone, MBL, using MBO as a CTA, the results of which are summarized in Table 3. As can be seen from the table, all MBL polymerizations in a [MBL]/I^{t}Bu] ratio of 1000 achieved quantitative monomer conversion in 72 h, regardless of the amount of the MBO added (from 0 to 100 equiv, relative to the catalyst I^{t}Bu). However, the resulting polymer MW decreased gradually from 25.2 kg/mol (run 1) to 16.3 kg/mol (run 6) with increasing the equiv of MBO from 0 to 100. Accordingly, the I^* values increased from 385% to 595%, featuring again a catalytic polymerization process.

DISCUSSION

The behavior of NHCs (IMes, I^{t}Bu, and TPT) as initiators or catalysts in the polymerization of MMA and MMBL was further investigated by density functional theory (DFT) calculations.[40] All geometries were localized in the gas phase. However, because polymerizations were performed in toluene and/or DMF, we performed single point energy calculations on the final geometries to take into account solvent effects. For monomers **1** (MMA and MMBL) we investigated the general reactivity shown in Scheme 3. Upon addition of an NHC molecule to monomer **1**, leading to zwitterionic adduct **2**, two possible scenarios were considered. In the first scenario, indicated in Scheme 3 as the enamine/dimerization pathway, there is an overall H-transfer from the Cα to the Cβ atom of **2**, leading to enamine **3**, followed by reaction of **3** with another monomer molecule, affording the dimerization product **4** with release of the NHC. In the second scenario, indicated in Scheme 3 as the polymerization pathway, the NHC adduct **2** directly reacts with another monomer molecule via classical 1,4-

dx.doi.org/10.1021/ja4088677 | J. Am. Chem. Soc. 2013, 135, 17925−17942

Table 2. Results of MMBL Polymerization by I^{t}Bu in the Presence of CTAs[a]

run no.	CTA	[CTA]/[I^{t}Bu]	[CTA]/[MMBL]	time (min)	conv. (%)	M_n (kg/mol)	PDI (M_w/M_n)	I^* (%)
1	–	0	0	1	>99	71.9	1.80	154
2	MIB	1	0.001	1	>99	82.5	2.17	134
3	MIB	10	0.01	1	>99	77.5	2.04	143
4	MIB	20	0.02	1	>99	80.0	2.10	139
5	MIB	50	0.05	1	>99	68.0	2.02	163
6	MIB	100	0.1	1	>99	68.7	1.94	161
7	MBO	1	0.001	1	>99	68.3	1.56	162
8	MBO	10	0.01	1	>99	47.7	1.47	232
9	MBO	20	0.02	1	>99	43.7	1.53	254
10	MBO	50	0.05	1	>99	31.5	1.33	352
11	MBO	100	0.1	1	>99	29.2	1.52	380
12	MBO	1000	1	1	>99	15.4	1.30	720
13	DMS	10	0.01	1	>99	50.4	1.95	220
14	DMS	1000	1	1	89	13.5	1.64	738
15	DMM	1	0.001	5	100	72.1	1.99	155
16	DMM	5	0.005	15	100	25.6	1.81	438
17	DMM	10	0.01	60	99	14.9	1.54	744
18	DMM	20	0.02	1080	>99	8.91	1.34	1244
19	DMM	50	0.05	2880	95[b]	6.13	1.26	1736
20	DMM	100	0.1	2880	80[c]	6.41	1.28	1398
21	DMM	1000	1	11520	98[d]	–	–	

[a]Carried out at ~25 °C in 4.5 mL DMF and 0.5 mL MMBL, where $[MMBL]_0$ = 0.936 M, [MMBL]/[I^{t}Bu] = 1000. [b]21% collected by precipitation in methanol. [c]6% collected by precipitation in methanol. [d]No precipitation in methanol.

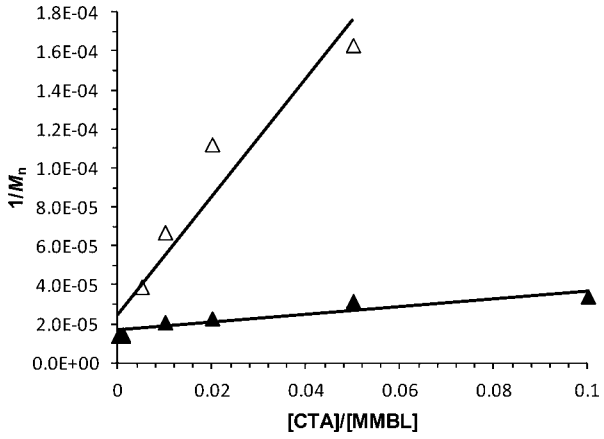

Figure 13. Plots of $1/M_n$ vs [CTA]/[M] (M = MMBL) for chain-transfer polymerization of MMBL by I^{t}Bu. CTA = DMM (Δ); MBO (▲).

conjugate addition to start the polymerization process. The mechanisms of the two pathways were investigated computationally both in toluene and DMF, considering all three NHCs, TPT, IMes, and I^{t}Bu, as depicted in Figure 1, and two monomers, the linear MMA and its cyclic analog MMBL.

Reactivity of NHCs toward MMA. Energetics relevant to the formation of the zwitterionic species **2** through NHC addition to monomer is summarized in Table 4. According to calculations, in either toluene or DMF the lowest energy NHC-MMA zwitterionic adduct **2** is that formed with IMes. Based on the data summarized in Table 4, the relative stability of the NHC-MMA adduct is IMes > TPT ≈ I^{t}Bu in toluene. This trend is not that expected based on the relative nucleophilicity of the NHCs (I^{t}Bu > IMes > TPT), but rather it correlates with the relative steric demand of the NHCs, as quantified by the buried volume (%V_{Bur}) of the NHC moiety[41] in the MMA adduct, I^{t}Bu = 36.1% ≈ TPT = 36.8% > IMes =32.3%. The rather large %V_{Bur} of TPT is consequence of the rotation of the phenyl rings next to the carbene C atom that assume a conformation nearly coplanar with the NHC ring. In IMes, the *ortho* Me groups prevent this rotation. On the other hand, the in-plane orientation of the phenyl rings in TPT allows extending the conjugation of the NHC ring, further stabilizing the free TPT molecule. A more polar solvent, DMF, appears to have a rather small impact on the energy values of the enamine/dimerization manifold reported in Table 4.

Zwitterionic adduct **2** is the branching point for dimerization vs polymerization. In the dimerization branch the first step is the H-transfer reaction to form enamine **3**, which reacts with a second MMA monomer to form the dimerization product **4** accompanied by NHC elimination (Scheme 3). Regarding the H-transfer step, owing to the expected high energy of the direct Cα to Cβ 1,2-shift, we focused on the two-step, bimolecular mechanism proposed in Scheme 4. In the first step, one H atom (H^1 in Scheme 4) is transferred from the Cα of a first NHC-MMA adduct to the Cβ of a second one, leading to the formation of the tightly bound ion pair **2′**. In the second step, the resulting intermediate (IM) **2′** undergoes a further H-transfer reaction where another H atom (H^2 in Scheme 4) is transferred from the Cα of the second moiety to the Cβ of the first moiety, generating two molecules of enamine product **3**. A similar two-step bimolecular proton-transfer mechanism was proposed for the Stetter reaction in nonprotic media involving 1,4-addition of aldehydes and Michael acceptors.[42]

The energetics of IM and TS species in Scheme 4 is reported in Table 4. Starting with TPT, the TPT-MMA adduct **2** undergoes a first H-transfer through TS **2**−**2′** with a barrier of ~11−12 kcal/mol, leading to the charged intermediate **2′**, roughly 14 kcal/mol below **2**. The second H-transfer, through TS **2′**−**3**, also has a barrier of ~13 kcal/mol and leads to the final enamine **3**, which is clearly more stable than the initial adduct **2** (by ~16 kcal/mol) and also of IM **2′** (by ~2 kcal/mol). The enamine product **3** can react with a further MMA

dx.doi.org/10.1021/ja4088677 | J. Am. Chem. Soc. 2013, 135, 17925−17942

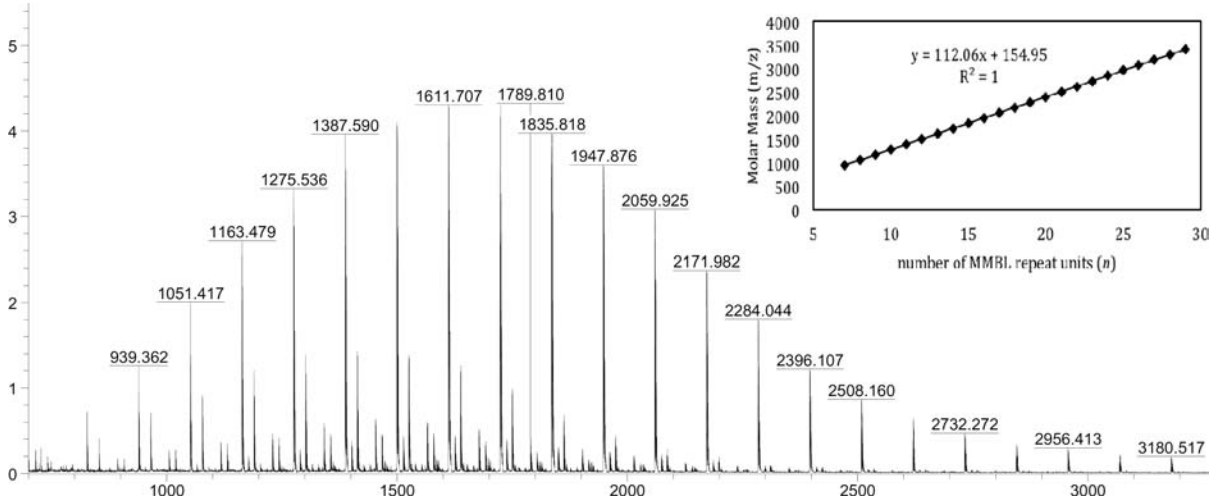

Figure 14. MALDI-TOF MS spectrum of low-molecular-weight MMBL oligomers produced by I^{t}Bu with DMM as the CTA. Inset: plot of m/z values of the major mass series vs the number of MMBL repeat units (n).

Table 3. Results of MBL Polymerization by I^{t}Bu in the Presence of MBO[a]

run no.	[MBL]/[I^{t}Bu]	[CTA]/[I^{t}Bu]	[CTA]/[MBL]	time (h)	conv. (%)	M_n (kg/mol)	PDI (M_w/M_n)	I^* (%)
1	1000	0	0	72	>99	25.2	1.50	385
2	1000	1	0.001	72	>99	24.0	1.52	404
3	1000	10	0.01	72	>99	22.7	1.50	427
4	1000	20	0.02	72	>99	21.7	1.45	447
5	1000	50	0.05	72	>99	18.5	1.46	524
6	1000	100	0.1	72	>99	16.3	1.77	595

[a]Carried out at ∼25 °C in 4.5 mL DMF and 0.5 mL MBL, $[MBL]_0$ = 1.14 M.

Scheme 3. Outlined Two Competing Reaction Pathways Involving Acrylic Monomers (MMA and MMBL) and NHCs

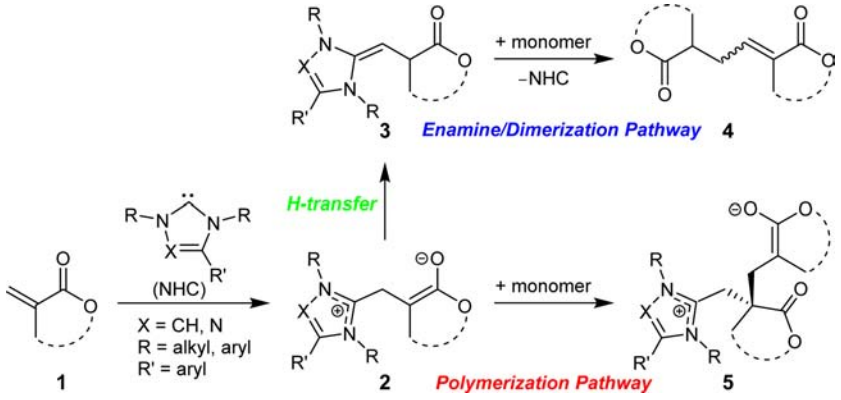

monomer via a classical monomer addition step (Scheme 5), through TS **3**–**3′** with a barrier of ∼21 kcal/mol, leading to the high energy IM **3′**. A final H-transfer step converts **3′** into dimerization product **4** with release of TPT and an energy gain of only 0.4 kcal/mol in toluene relative to **3** and basically thermo-neutral in DMF. These yielded mechanistic features for the TPT-catalyzed MMA dimerization, including bimolecular (or intermolecular) proton transfer and the rate-limiting step being the addition of the enamine intermediate to the second MMA (which exhibits the highest activation barrier of ∼21 kcal/mol), agreeing well with the most recent results of experimental mechanistic studies by Matsuoka and co-workers.[43]

Moving to IMes, we found that the energy profiles of IMes are rather similar to those of TPT, with all TSs being of reasonably close energy. However, there is a relevant difference in the relative stability of enamine **3** with respect to product **4**. In fact, according to calculations, enamine **3** is the most stable species in the IMes promoted reactivity of MMA, whereas for TPT the most stable species is dimer **4**. This difference suggests that in the presence of IMes MMA dimerization is unfavored because dimer **4** is 2.3 kcal/mol higher in energy than enamine **3**. Finally, I^{t}Bu is unable to promote MMA dimerization, due to the high-energy barrier for the first H-transfer, 27 kcal/mol, as a result of the greater steric hindrance of I^{t}Bu in the I^{t}Bu-MMA adduct. To reaffirm this reasoning, we also performed the calculations with 1,3-di-isopropylimidazolin-2-ylidene (I^{i}Pr) and found the energy barrier for its H-transfer process is ∼11 kcal/mol lower than that with I^{t}Bu, in agreement with the steric difference between the two NHC-MMA adducts. Overall, all

dx.doi.org/10.1021/ja4088677 | J. Am. Chem. Soc. 2013, 135, 17925–17942

Table 4. Energy of the Species Shown in Schemes 3−5, with MMA as the Monomer[a]

	IMes	I^{t}Bu	TPT	IMes	I^{t}Bu	TPT
		toluene			DMF	
1	0	0	0	0	0	0
2	−7.3	0.4	−2.9	−8.1	−1.4	−1.2
			Enamine/Dimerization			
2−2′	4.3	27.4	9.4	6.6	27.7	10.0
2′	−12.4	16.3	−17.2	−10.3	15.3	−15.4
2′−3	−5.9	29.0	−3.8	−1.4	29.9	−1.7
3	−21.9	−5.3	−19.2	−19.9	−4.4	−18.8
3−3′	−2.5	9.9	2.1	−2.0	9.7	1.9
3′	−6.1	6.0	0.9	−7.7	5.4	0.1
4	−19.6	−19.6	−19.6	−18.8	−18.8	−18.8
			Polymerization			
2−5	−3.7	3.6	4.5	−5.5	0.6	2.8
5	−9.4	0.4	−3.6	−12.4	−4.0	−6.1

[a]Energy is reported in kcal/mol and relative to NHC + free MMA. **X**−**Y** denotes transition state (TS) from species **X** to species **Y**.

these computational results are consistent with our experimental findings described in the Results section.

Next we examined the behavior of the NHC-MMA zwitterionic adduct **2** in promoting polymerization, through addition of a second MMA to **2** (Scheme 3). Analysis of the data reported in Table 4 indicates that addition of a second MMA molecule to any of the NHC-MMA adducts, through TS **2**−**5**, is a rather feasible process with a barrier smaller than 10 kcal/mol, whatever NHC and solvent is considered. The product of the first propagation step (i.e., the second monomer addition), **5**, is only slightly more stable than the starting species, making addition of MMA to the NHC-MMA adduct reversible. Comparison of the H-transfer with the polymerization pathway, that is TS **2**−**2′** vs **2**−**5**, indicates that for TPT the barrier for the second monomer addition, roughly 4−7 kcal/mol (depending on solvent), is about one-half of that for the H-transfer converting **2** into enamine species **3** and finally the dimer product **4**. However, the overall product of the H-transfer, dimer **4**, is the thermodynamically more stable species, in agreement with the experimental evidence that the TPT−MMA adduct undergoes H-transfer and than dimerizes. Moving to IMes, the energy profiles of TPT and IMes promoted polymerization are again rather similar, with the difference being that IMes, in agreement with the experimental results, stops at the more stable enamine product **3** without reaching to dimer **4**. These conclusions are independent of the solvent polarity.

Lastly for I^{t}Bu, the computational data are rather different from those for IMes and TPT and further are different in toluene and in DMF. In fact, in toluene the H-transfer barrier leading to enamine **3** is too high (27 kcal/mol), preventing the reaction to move along this pathway, while the MMA addition barrier starting polymerization is low, but the addition product **5** is not stable. As consequence, I^{t}Bu is practically inactive toward MMA in toluene. Moving to DMF, the H-transfer reaction along the enamine/dimerization pathway is still inaccessible, but the I^{t}Bu-MMA adduct can add another monomer with a negligible energy barrier leading to stable addition product **5**, −4.0 kcal/mol below MMA + I^{t}Bu. Obviously, the higher stability of the addition product (the zwitterionic propagating species) along the polymerization pathway in the more polar DMF is due to the electrostatic stabilization. Again, these computational data are in agreement with the experiments that showed that I^{t}Bu does not react with MMA in toluene, but it polymerizes MMA in DMF (vide supra).

Termination Reaction in MMA Polymerization. In this section we discuss a possible mechanism of termination operative in the MMA polymerization promoted by I^{t}Bu in DMF. We investigated the pathway proposed in Scheme 6 and used two methyl groups to model the chain segment connecting the cationic and anionic moieties of the growing chain in the starting zwitterionic species (P = CH_3 in Scheme 6). This termination reaction corresponds to a H-transfer from the $-CH_2-$ group bound to the I^{t}Bu to the enolate C atom of the chain end, through a TS with a barrier of 8.8 kcal/mol, leading to the termination product (an enamine) with chain ends shown in the Scheme 6. The resulting termination product is 13.1 kcal/mol lower in energy relative to the starting zwitterionic propagation species considered. However, the barrier for the propagation species to add another MMA (∼2 kcal/mol) is much lower than that for this termination step, explaining why a medium-high MW polymer (33.2 kg/mol) is achieved by I^{t}Bu in DMF. We also considered the possibility of the enamine termination product to add another MMA molecule, but the energy barrier for this addition is calculated to be 26.8 kcal/mol. Overall, these computational results are in agreement with experimental evidence for the observed enamine chain ends by ^{1}H NMR and MALDI-TOF MS (vide supra), and the MMA polymerization is noncatalytic (i.e., the terminated enamine species is not longer active for further MMA additions).

Reactivity of NHCs toward MMBL. The same competing enamine/dimerization and polymerization pathways were explored for MMBL, the results of which are reported in Table 5. The overall scenario emerging from Table 5 is rather

Scheme 4. Proposed Two-Step Bimolecular H-Transfer Mechanism Involving the Ion Pair Intermediate

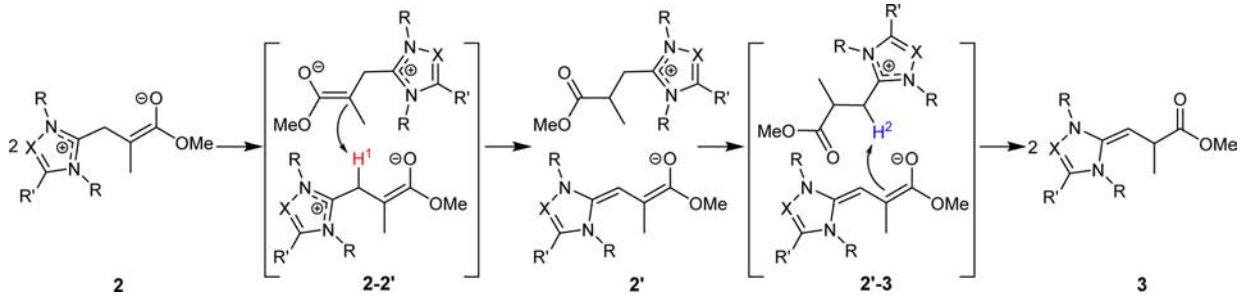

dx.doi.org/10.1021/ja4088677 | J. Am. Chem. Soc. 2013, 135, 17925−17942

Scheme 5. Energetics (kcal/mol) of MMA Dimerization Catalyzed by TPT

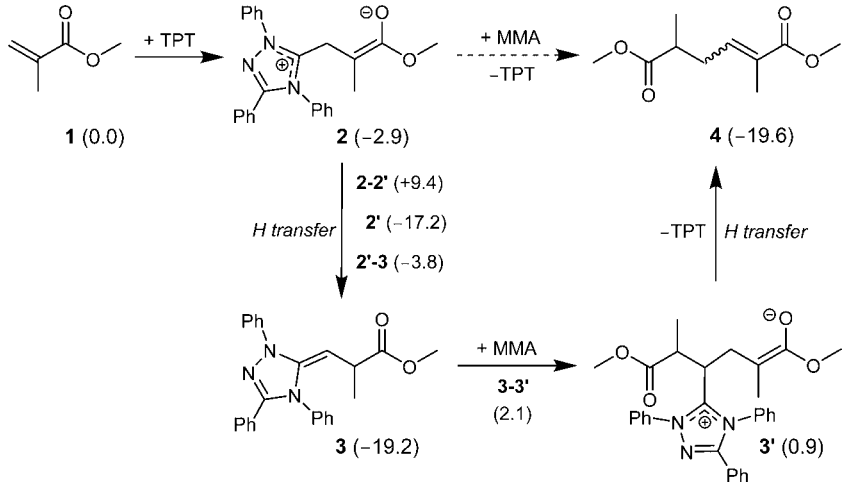

Scheme 6. Energetics for the Species Involved in the Termination Step of MMA Polymerization by I^{t}Bu in DMF[a]

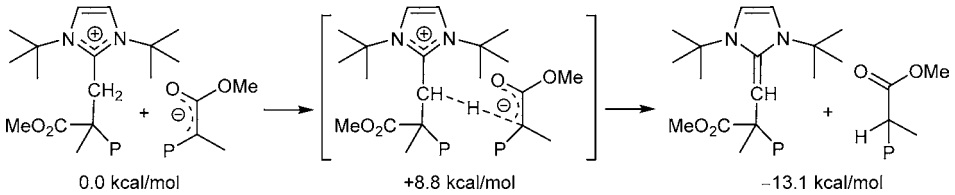

[a]Note the cationic and anionic moieties of the growing chain are connected through two P sites.

similar to that discussed above for MMA; hence, the details are not discussed here, illuminating instead the differences.

Table 5. Energy of the Species Shown in Schemes 3 and 4, with MMBL as the Monomer[a]

	IMes	I^{t}Bu	TPT	IMes	I^{t}Bu	TPT
		toluene			DMF	
1	0	0	0	0	0	0
1–2	6.1	14.4	7.1	7.8	12.9	8.7
2	−8.8	−0.6	−2.7	−9.9	−3.1	−2.6
		Enamine/Dimerization				
2–2′	4.1	24.5	6.7	5.3	24.8	8.7
2′	−18.6	4.7	−19.3	−15.6	4.8	−15.6
2′–3	−10.8	25.0	−6.8	−6.3	27.7	−3.0
3	−23.2	−5.0	−19.3	−20.2	−4.3	−18.6
3–3′	−7.0	9.6	−2.0	−6.8	−2.9	7.6
3′	−10.9	3.8	−5.1	−13.7	−1.2	−8.1
4	−18.7	−18.7	−18.7	−18.4	−18.4	−18.4
		Polymerization				
2–5	−4.8	1.8	0.7	−4.9	0.7	2.1
5	−10.0	−4.5	−7.0	−10.4	−6.7	−7.2

[a]Energy is reported in kcal/mol and relative to NHC + free MMBL.

In short, the energetic numbers reported in Table 5 indicate again that I^{t}Bu behaves differently with respect to IMes and TPT also in case of MMBL. The energy of TS **1–2** for the formation of the zwitterionic adduct **2** with I^{t}Bu is roughly 7–8 kcal/mol higher in energy than that with IMes and TPT, and the energy barrier for the H-transfer step along the enamine/dimerization pathway is roughly 20 kcal/mol higher than that calculated for IMes and TPT. This barrier is large enough to conclude that I^{t}Bu is unable to promote reactivity along the enamine/dimerization pathway for MMBL either. Conversely, IMes and TPT result in a low energy barrier for the first H-transfer step, ∼9–15 kcal/mol, and in stable products, ∼18–23 kcal/mol below NHC + free MMBL, in both toluene and DMF. However, for both IMes and TPT, enamine **3** is more stable than dimer **4**, which is in agreement with the experimental evidence that no dimer of MMBL is formed whatever NHC is considered.

Next we focused on the first step of the polymerization pathway, in which the NHC-MMBL zwitterionic adduct **2** attacks the exocyclic CH_2 group of a MMBL molecule via 1,4-conjugate addition. As for MMA, the most stable NHC-monomer adduct is the one with IMes in both solvents, followed by the adduct with TPT in toluene and the one with I^{t}Bu in DMF. Again, the energy barrier for the NHC-MMBL adduct **2** to add another monomer molecule, through TS **2–5**, is quite small with all the three NHCs considered herein, 2.4 kcal/mol for I^{t}Bu, 3.4 kcal/mol for TPT and 4.0 kcal/mol for IMes in toluene. A similar trend is seen in DMF. These computational data would suggest that all the three NHCs considered could promote MMBL polymerization. In fact, experimentally I^{t}Bu promotes extremely rapid polymerization of MMBL in both solvents, especially in DMF, and IMes also initiates MMBL polymerization in either solvent, albeit with much lower activity than I^{t}Bu, while TPT is inactive for MMBL polymerization in DMF, but in toluene it is active with even lower activity than IMes (vide supra).

The different reactivity trend toward MMBL polymerization among the three NHCs can be rationalized by relative aptitude in competing H-transfer and monomer-addition reactions involving the zwitterionic adduct **2**. Specifically, in the case of I^{t}Bu, the H-transfer reaction barrier along the enamine/dimerization pathway is much larger than the barrier along

dx.doi.org/10.1021/ja4088677 | J. Am. Chem. Soc. 2013, 135, 17925–17942

Scheme 7. A Possible Alternative Initiation and Propagation Pathway for the MMBL Polymerization by NHCs, Where the NHC Serves as a Base

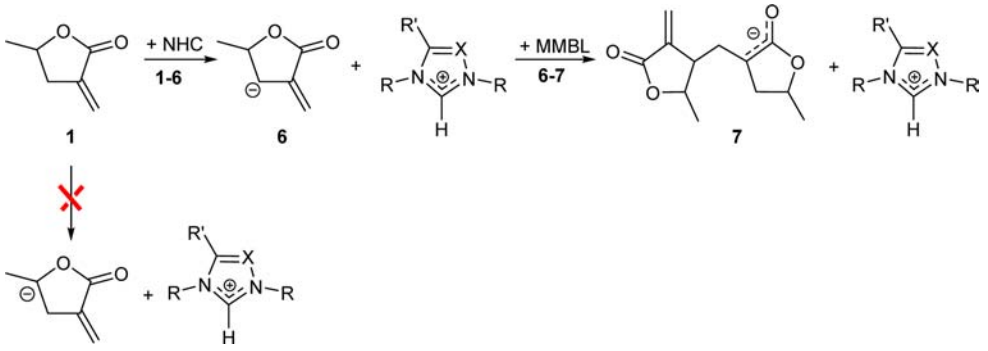

the polymerization pathway, permitting the reactivity only along the polymerization pathway and shutting down the enamine/dimerization pathway. In case of TPT and IMes, both the H-transfer reaction along the enamine/dimerization pathway and the MMBL addition along the polymerization pathway can occur, in principle, since they both show relatively low-energy barriers. Although the barrier for the polymerization step is clearly lower than the barrier for the H-transfer, the most remarkable difference between the two pathways is in the stability of the products. In fact, the MMBL addition product **5** along the polymerization pathway is roughly 10 kcal/mol less stable than the H-transfer reaction product enamine **3**. Since MMBL addition from **2** to **5** can be reversed, the system can accumulate into the most stable enamine **3**, reducing the polymerization activity. However, the system with IMes is more biased toward the polymerization pathway, since the preference for the polymerization pathway, measured by the energy difference between TSs **2**−**2′** and **2**−**5**, increases by roughly 2 kcal/mol on going from TPT to IMes. This analysis explains the experimental evidence that the MMBL polymerization activity with IMes is somewhat between I^{t}Bu and TPT activities.

As the other general trend for I^{t}Bu and IMes, comparison of the energetics in toluene with that in DMF indicates that in the more polar DMF solvent the NHC-monomer adduct **2** and the product **5** tend to be more stable, and the energy of the TS involved in the monomer addition becomes slightly lower; this observation is in agreement with the greater experimental activity of these two NHCs in DMF. However, the trend for TPT is opposite in the two solvents, in agreement with the experimental results showing that TPT is inactive for MMBL polymerization in DMF.

Considering that the data reported in Table 5 indicate that the TS **1**−**2** for the formation of I^{t}Bu-MMBL adduct is the highest in energy, and yet the experimental data showed that I^{t}Bu is the most active in the MMBL polymerization, we explored the alternative initiation pathway outlined in Scheme 7. In this pathway, an NHC serves as a strong base to abstract a proton of MMBL, forming a high-energy, highly reactive anion that initiates rapid polymerization. We examined abstraction of both β- and γ-protons of MMBL and found that abstraction of β-H costs 14.3 kcal/mol, while abstraction of γ-H costs 49.5 kcal/mol. Accordingly, the much preferred β-H abstraction generates an initiating species, anionic monomer **6** stabilized by electronic delocalization over the extend π-conjugated orbitals (Scheme 7). The first propagation step consists of addition of **6** to another MMBL molecule. The energetics of the alternative mechanism shown in Scheme 7 in DMF is reported in Table 6.

Table 6. Energy of the Species Shown in Scheme 7 [a]

	IMes	I^{t}Bu	TPT
		DMF	
1	0	0	0
1−**6**	17.6	16.7	20.1
6	17.7	14.3	32.0
6−**7**[b]	−	−	−
7	−4.4	−7.8	+9.9

[a]Energy is reported in kcal/mol and relative to NHC + free MMBL. [b]No energy barrier.

The rate-determining step for all the three NHCs is the formation of the active species **6** through abstraction of the β-proton from MMBL by an NHC base. In fact, once the anion **6** is formed, it can add a monomer molecule without any energy barrier. Thus, the highest energy barrier in the reaction pathway of Scheme 7, through TS **1**−**6** is roughly 17−20 kcal/mol for the three NHC systems. Comparing the energy of TS **1**−**6** in Table 6, and TS **1**−**2** in Table 5, it is clear that the mechanism of Scheme 7 is highly unfavored relative to the mechanism of Scheme 3 for both IMes and TPT. In fact, the energy barrier of TS **1**−**2** is 9.8 and 11.4 kcal/mol lower than TS **1**−**6** for IMes and TPT, respectively. For I^{t}Bu, the difference is lower, but with TS **1**−**2** being 3.8 kcal/mol lower in energy than TS **1**−**6**, the proton abstraction pathway outlined in Scheme 7 is still less favorable than the nucleophilic addition pathway outlined in Scheme 3. This conclusion is further reaffirmed by the experiment that showed no reaction took place between I^{t}Bu and γ-valerolactone (1−5 equiv), a suitable nonpolymerizable monomer model possessing even more acidic protons than the monomer MMBL.

Termination Reaction in MMBL Polymerization. To shed light on the termination mechanism operating in the MMBL polymerization promoted by I^{t}Bu, we explored three possible termination pathways. The first possible mechanism, consisting of S_N2 nucleophilic substitution reaction where the NHC is the leaving group, would lead to formation of a cyclic polymer, according to the two possible pathways schematized in Scheme 8. In the mechanism of Scheme 8a the nucleophile center is the Cα atom of the last MMBL unit and a new C−C bond is formed in **10**, while in that of Scheme 8b the nucleophile center is the enolate oxygen, where the major negative charge is localized, and an O−C bond is formed in **11**.

dx.doi.org/10.1021/ja4088677 | J. Am. Chem. Soc. 2013, 135, 17925−17942

Scheme 8. Examined Possible Termination Pathways to a Cyclic Polymer

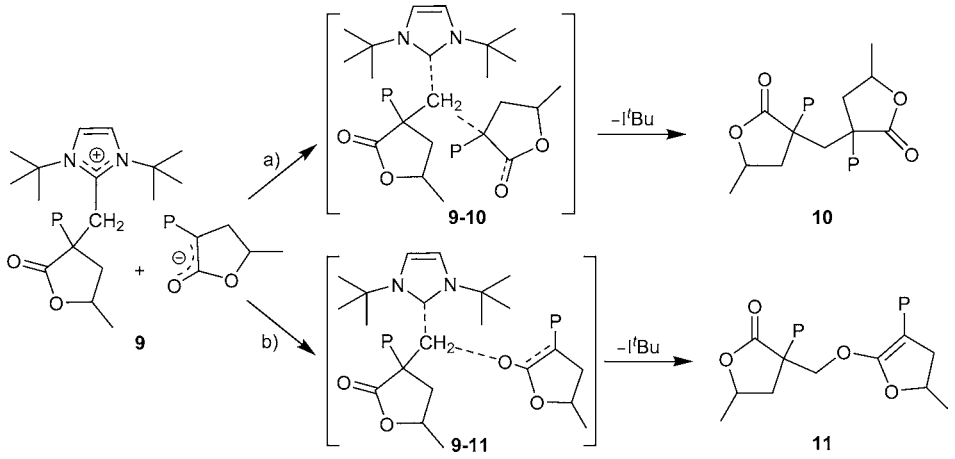

Scheme 9. Possible Termination Pathways Through H-Transfer and Enamine Intermediate 13

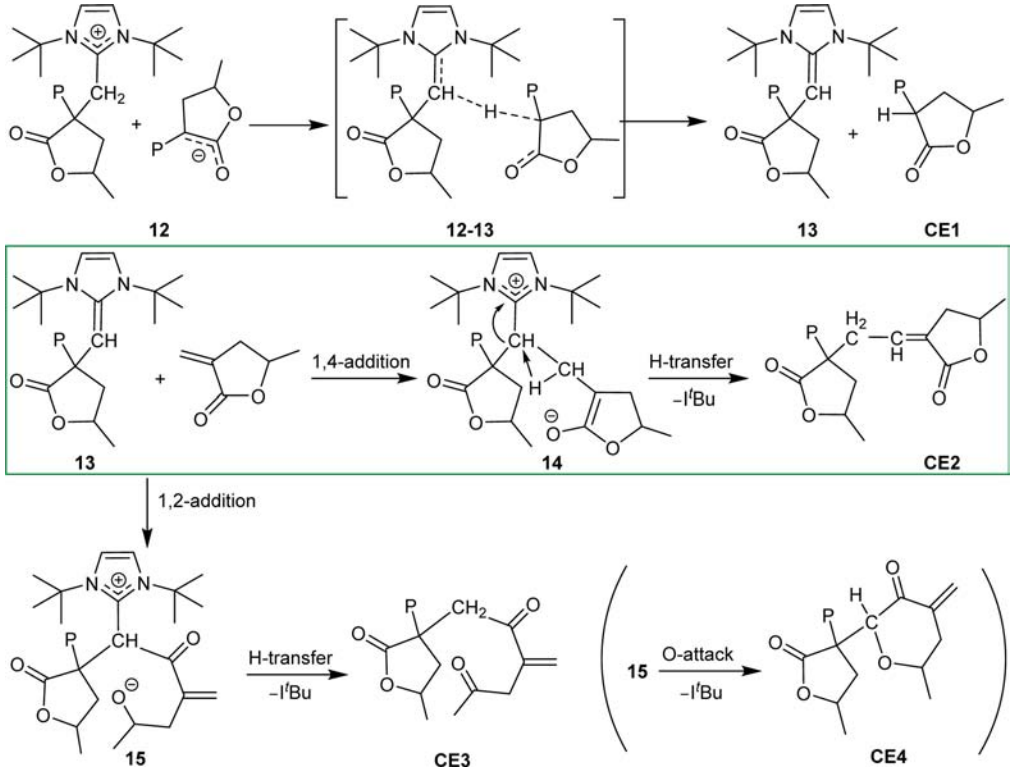

In both cases two methyl groups were used to model the chain segment connecting the cationic and anionic moieties of the growing chain in the starting zwitterionic species **9** (P = CH_3 in Scheme 8). This treatment avoids the complication of modeling a long polymer chain joining the two reacting moieties. Nevertheless, both pathways showed very high energy, with the mechanism of Scheme 8a resulting in a barrier higher than 40 kcal/mol, while for the mechanism in Scheme 8b the calculated barrier is ∼50 kcal/mol, thus effectively ruling out these termination pathways. This analysis is consistent with our experimental result that showed no cyclic polymer formation.

Keeping in mind the feasibility of H-transfer reactions with these systems, we investigated the second possible chain termination pathways outlined in Scheme 9 starting from the active zwitterionic propagating species **12**. The relative energetics of all species involved are summarized in Table 7.

Table 7. Energy of the Species Shown in Scheme 9 [a]

	I^{t}Bu toluene	I^{t}Bu DMF
12	0	0
12–13	9.9	10.8
13 + CE1	−12.8	−10.7
13–14	2.1	−0.2
CE2	−31.2	−30.7
13–15	8.5	9.7
15	6.2	6.7
15–CE3	>30	>30
15–CE4	39.6	42.1
CE3	−18.2	−17.4
CE4	−9.8	−7.6

[a]Energy is in kcal/mol.

dx.doi.org/10.1021/ja4088677 | J. Am. Chem. Soc. 2013, 135, 17925−17942

The first step of the termination sequence corresponds to a H-transfer from the $-CH_2-$ group bound to the I^{t}Bu to the enolate C atom of the chain end in **12**, through TS **12**−**13** with a barrier of roughly 10 kcal/mol, leading to enamine type species **13** and chain end **CE1** (Scheme 9). Chain end **CE1** could not be identified by NMR, due to its overlap with the main polymer peaks, but the enamine moiety in **13** can be identifiable by NMR and MALDI-TOF MS (vide supra). Interestingly, this reaction also allows for formation of an enamine-type structure with I^{t}Bu, a step not possible by direct H-transfer between two I^{t}Bu-MMBL adducts (cf., Table 5). Enamine species **13** can further react with another MMBL molecule through a classical 1,4-addition to give IM **14**, through TS **13**−**14** with an energy barrier of also roughly 10 kcal/mol (in DMF), and finally chain end, **CE2**, through a second H-transfer step. Alternatively, the reaction of enamine species **13** with another MMBL could proceed via a less favored 1,2-addition pathway to give IM **15**, through TS **13**−**15** with a barrier of roughly 15 kcal/mol. Subsequently, IM **15** could undergo another H-transfer or nucleophilic substitution by the oxygen atom, leading respectively to chain end **CE3** or **CE4**. However, the TSs for the final nucleophilic attack or H-transfer have been calculated to be more than 40 kcal/mol higher in energy, making this termination pathways unlikely.

We further investigated the third possible chain termination pathway through chain transfer to monomer as outlined in Scheme 10. In this case the reactive enolate chain end abstracts

Scheme 10. Proposed Chain Termination Pathway via Chain Transfer to Monomer

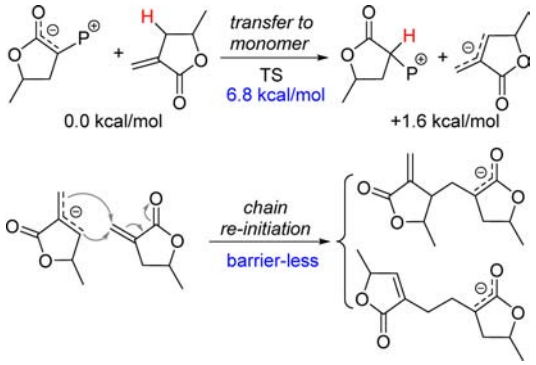

a proton from the β-C of the monomer, with a barrier of only 6.8 kcal/mol. As result, the old chain P still has the $[NHC]^+$ attached to it as the polymeric counterion, paired with the monomer anion that re-initiates a new chain, effecting a catalytic polymerization (cf., Schemes 1 and 10). Although the overall reaction seems to be not favored (i.e., the products are 1.6 kcal/mol higher in energy vs the reactants), it is worth noting that the generated strong nucleophile (anionic monomer) can readily add a monomer without any energy barrier (Scheme 10), leading to formation of more favored products (with an energy gain of 20.5 kcal/mol for the addition of the second monomer).

Overall, after having explored several different termination pathways, we found that only H-transfer/enamine addition and transfer to monomer pathways are energetically feasible. Between these two pathways, the chain termination, through an H-transfer reaction to generate the enamine type intermediate **13**, followed by an 1,4-addition to another MMBL molecule and subsequent second H-transfer to finally chain end **CE2** and release of the NHC catalyst (green box, Scheme 9), has an activation energy barrier of slightly higher than 10 kcal/mol, while the chain termination through chain transfer to monomer (Scheme 10) has an energy barrier of <7 kcal/mol. On the basis of experimental results (vide supra), the H-transfer/enamine addition termination is effective only with a high NHC loading (e.g., the NMR signals relative to **CE1** and **CE2** were found with a $[MMBL]_0/[I^tBu]_0$ ratio of 5:1 or similar). In other instances (e.g., high $[MMBL]_0/[I^tBu]_0$ ratios) the chain-transfer termination to monomer, which is more favored from an energetic point of view (6.8 vs 10 kcal/mol), takes place. Finally, these activation energies associated with the chain termination events are compared to a barrier of only ∼3 kcal/mol for the active propagation species to add another MMBL, thereby explaining why a rather high MW polymer (up to ∼90 kg/mol) can be achieved by I^{t}Bu.

CONCLUSIONS

In summary, this contribution presented a full account of our combined experimental and theoretical/computational investigations into the recently discovered NHC-mediated organocatalytic conjugate-addition polymerization of acrylic monomers, represented by the most common linear monomer MMA and its cyclic analog MMBL. Remarkably, there exhibits an exquisite selectivity of the NHC structure for the three types of reactions with the substrate it promotes: enamine formation, dimerization, and polymerization. This organopolymerization is especially effective for the biomass-derived renewable methylene butyrolactones such as MMBL, thus quantitatively converting a large excess of monomer (e.g., 10 000 equiv or 0.01 mol % NHC loading) into the corresponding bioplastics within 5 min and achieving an exceptionally high maximum turnover frequency up to 122 s^{-1}. Unique chain termination mechanisms have been revealed, which account for the production of relative high-molecular-weight linear polymers and the catalytic nature of this polymerization. Computational studies have provided mechanistic insights into reactivity and selectivity between two competing pathways for each NHC-monomer zwitterionic adduct: enamine formation/dimerization through proton transfer vs polymerization through conjugate addition.

Key conclusions drawn from the herein described study are listed as follows:

(1) IMes reacts with MMA to form exclusively the single-monomer addition product, enamine, or deoxy-Breslow intermediate **3**. This reaction proceeds through a proposed two-step, bimolecular mechanism involving initial facile formation of the zwitterionic IMes-MMA adduct **2**, followed by proton transfer between the two molecules of **2** to generate a tightly bound ion pair intermediate which leads to the final enamine **3** after an additional proton-transfer reaction within the ion pair. The IMes-based enamine is the most stable enamine of the current NHC series, and it does not react further with monomer to form the dimerization product **4**, due to the fact that dimer **4** is calculated to be 2.3 kcal/mol higher in energy than enamine **3**.

(2) TPT catalyzes efficient dimerization of MMA to form dimer **4** in good yields. In contrast to IMes, TPT-derived enamine **3** can react further with MMA through a conjugate-addition step followed by a proton-transfer step, affording dimer **4**. Energetically, the addition of

dx.doi.org/10.1021/ja4088677 | J. Am. Chem. Soc. 2013, 135, 17925−17942

enamine **3** to the second MMA has the highest energy barrier of ∼20 kcal/mol, thus a rate-limiting step of the dimerization process, and for TPT the most stable species is dimer **4**, thus providing an overall thermodynamic driving force for the dimerization.

(3) I^{t}Bu does not react with MMA in toluene to form the corresponding zwitterionic adduct **2**, which is unstable due to the large buried volume %V_{Bur} of I^{t}Bu, and is also unable to promote MMA dimerization, due to the high-energy barrier (27 kcal/mol) for the first proton transfer on going from zwitterionic adduct **2** to enamine intermediate **3**.

(4) I^{t}Bu polymerizes MMA to PMMA with a medium-high-molecular-weight (M_n = 33.2 kg/mol) in the polar solvent DMF, due to the increased stability of the first zwitterionic adduct and the subsequent zwitterionic active propagating species in DMF as well as a relatively low-energy barrier (∼2 kcal/mol) for subsequent conjugate additions of propagating species to monomer. The chain termination reaction, through proton transfer from the $-CH_2-$ group bound to the I^{t}Bu to the enolate C atom of the growing chain end, generates an enamine chain end, which is incapable of reacting further with monomer. Hence, the MMA polymerization promoted by I^{t}Bu in DMF is noncatalytic.

(5) For MMBL, the NHC promotes no dimerization but polymerization, with the polymerization activity being highly sensitive to the NHC structure and the solvent polarity. Again, I^{t}Bu is unable to promote MMBL reactivity along the enamine/dimerization pathway, due to the high-energy barrier (25 kcal/mol in toluene or 28 kcal/mol in DMF) for the first proton transfer on going from zwitterionic adduct **2** to enamine intermediate **3**. For IMes and TPT, the energy barrier for proton transfer is much lower, but enamine **3** is more stable than dimer **4**, thus no dimer formation. On the other hand, the energy barrier for the polymerization pathway via conjugate addition of the NHC-MMBL zwitterionic adduct **2** to monomer is quite small with all the three NHCs considered, 2.4 kcal/mol for I^{t}Bu, 3.4 kcal/mol for TPT, and 4.0 kcal/mol for IMes in toluene (a similar trend is also seen in DMF). The different reactivity trend toward MMBL polymerization among the three NHCs, I^{t}Bu > IMes > TPT, can be rationalized by the relative aptitude in competing proton-transfer and conjugate-addition reactions involving zwitterionic adduct **2**, the branching point of the two reactivity pathways.

(6) I^{t}Bu rapidly polymerizes MMBL in DMF to PMMBL, thus quantitatively converting 1000−3000 equiv of monomer in 1 min or 10 000 equiv in 5 min. The molecular weight of the resulting polymer remains nearly constant in a narrow range of M_n = 70−85 kg/mol regardless of the [MMBL]/[I^{t}Bu] ratio employed as long as it is higher than 800, due to substantial internal chain transfer that also results in high initiator efficiency values up to 1600%. Two chain-transfer termination pathways have been identified, with the H-transfer/enamine addition termination being present only with a high catalyst loading and the more energetically favored chain transfer to monomer being effective in other instances, but both pathways provide internal chain-transfer routes for catalytic polymerization. Addition of a suitable organic acid such as MBO can also promote external catalytic chain-transfer polymerization.

■ ASSOCIATED CONTENT

Supporting Information

Full experimental and computational details. This material is available free of charge via the Internet at http://pubs.acs.org.

■ AUTHOR INFORMATION

Corresponding Authors

luigi.cavallo@kaust.edu.sa
eugene.chen@colostate.edu

Notes

The authors declare no competing financial interest.

■ ACKNOWLEDGMENTS

This work was supported by the National Science Foundation (NSF-1012326 and NSF-1300267) for the study carried out at Colorado State University. L.C. thanks the HPC team of Enea (www.enea.it) for using the ENEA-GRID and the HPC facilities CRESCO (www.cresco.enea.it) in Portici, Italy.

■ REFERENCES

(1) Selected recent reviews: (a) Wende, R. C.; Schreiner, P. R. *Green Chem.* **2012**, *14*, 1821−1849. (b) Jacobsen, E. N.; MacMillan, D. W. C. *Proc. Natl. Acad. Sci. U.S.A.* **2010**, *107*, 20618−20619. (c) Grondal, C.; Jeanty, M.; Enders, D. *Nat. Chem.* **2010**, *2*, 167−178. (d) MacMillan, D. W. C. *Nature* **2008**, *455*, 304−308. (e) Houk, K. N.; List, B. Eds. Asymmetric Organocatalysis, special edition issue, *Acc. Chem. Res.* **2004**, *37*, 487−631.

(2) Selected recent reviews: (a) Ryan, S. J.; Candish, L.; Lupton, D. W. *Chem. Soc. Rev.* **2013**, *42*, 4906−4917. (b) Grossmann, A.; Enders, D. *Angew. Chem., Int. Ed.* **2012**, *51*, 314−325. (c) Bugaut, X.; Glorius, F. *Chem. Soc. Rev.* **2012**, *41*, 3511−3522. (d) Biju, A. T.; Kuhl, N.; Glorius, F. *Acc. Chem. Res.* **2011**, *44*, 1182−1195. (e) Dröge, T.; Glorius, F. *Angew. Chem., Int. Ed.* **2010**, *50*, 6940−6952. (f) Chiang, P.-C.; Bode, J. W. In *RSC Catalysis Series*; Royal Society of Chemistry: Cambridge, 2010, pp 399−435. (g) Moore, J. L.; Rovis, T. *Top. Curr. Chem.* **2009**, *291*, 77−144. (h) Hahn, F. E.; Jahnke, M. C. *Angew. Chem., Int. Ed.* **2008**, *47*, 3122−3172. (i) Nair, V.; Vellalath, S.; Babu, B. P. *Chem. Soc. Rev.* **2008**, *37*, 2691−2698. (j) Marion, N.; Díez-González, S.; Nolan, S. P. *Angew. Chem., Int. Ed.* **2007**, *46*, 2988−3000. (k) Enders, D.; Niemeier, O.; Henseler, A. *Chem. Rev.* **2007**, *107*, 5606−5655. (l) Bourissou, D.; Guerret, O.; Gabbaï, F. P.; Bertrand, G. *Chem. Rev.* **2000**, *100*, 39−91.

(3) (a) Nyce, G. W.; Glauser, T.; Connor, E. F.; Möck, A.; Waymouth, R. M.; Hedrick, J. L. *J. Am. Chem. Soc.* **2003**, *125*, 3046−3056. (b) Connor, E. F.; Nyce, G. W.; Myers, M.; Möck, A.; Hedrick, J. L. *J. Am. Chem. Soc.* **2002**, *124*, 914−915. (c) Nederberg, F.; Connor, E. F.; Möller, M.; Glauser, T.; Hedrick, J. L. *Angew. Chem., Int. Ed.* **2001**, *40*, 2712−2715.

(4) Selected reviews: (a) Brown, H. A.; Waymouth, R. M. *Acc. Chem. Res.* **2013**, DOI: 10.1021/ar400072z. (b) Fèvre, M.; Pinaud, J.; Gnanou, Y.; Vignolle, J.; Taton, D. *Chem. Soc. Rev.* **2013**, *42*, 2142−2172. (c) Kiesewetter, M. K.; Shin, E. J.; Hedrick, J. L.; Waymouth, R. M. *Macromolecules* **2010**, *43*, 2093−2107. (d) Kamber, N. E.; Jeong, W.; Waymouth, R. M.; Pratt, R. C.; Lohmeijer, B. G. G.; Hedrick, J. L. *Chem. Re.* **2007**, *107*, 5813−5840.

(5) (a) Jeong, W.; Shin, E. J.; Culkin, D. A.; Hedrick, J. L.; Waymouth, R. M. *J. Am. Chem. Soc.* **2009**, *131*, 4884−4891. (b) Culkin, D. A.; Jeong, W.; Csihony, S.; Gomez, E. D.; Balsara, N. P.; Hedrick, J. L.; Waymouth, R. M. *Angew. Chem., Int. Ed.* **2007**, *46*, 2627−2630. (c) Dove, A. P.; Li, H.; Pratt, R. C.; Lohmeijer, B. G. G.; Culkin, D. A.; Waymouth, R. M.; Hedrick, J. L. *Chem. Commun.* **2006**, 2881−2883. (d) Coulembier, O.; Dove, A. P.; Pratt, R. C.; Sentman, A. C.; Culkin, D. A.; Mespouille, L.; Dubois, P.; Waymouth, R. M.; Hedrick, J. L.

Angew. Chem., Int. Ed. **2005**, *44*, 4964−4968. (e) Csihony, S.; Culkin, D. A.; Sentman, A. C.; Dove, A. P.; Waymouth, R. M.; Hedrick, J. L. *J. Am. Chem. Soc.* **2005**, *127*, 9079−9084.
(6) (a) Shin, E. J.; Brown, H. A.; Gonzalez, S.; Jeong, W.; Hedrick, J. L.; Waymouth, R. M. *Angew. Chem., Int. Ed.* **2011**, *50*, 6388−6391. (b) Sen, T. K.; Sau, S. Ch.; Mukherjee, A.; Modak, A.; Mandal, S. K.; Koley, D. *Chem. Commun.* **2011**, *47*, 11972−11974. (c) Kamber, N. E.; Jeong, W.; Gonzalez, S.; Hedrick, J. L.; Waymouth, R. M. *Macromolecules* **2009**, *42*, 1634−1639. (d) Jeong, W.; Hedrick, J. L.; Waymouth, R. M. *J. Am. Chem. Soc.* **2007**, *129*, 8414−8415.
(7) (a) Raynaud, J.; Absalon, C.; Gnanou, Y.; Taton, D. *Macromolecules* **2010**, *43*, 2814−2823. (b) Raynaud, J.; Ottou, W. N.; Gnanou, Y.; Taton, D. *Chem. Commun.* **2010**, *46*, 3203−3205. (c) Raynaud, J.; Absalon, C.; Gnanou, Y.; Taton, D. *J. Am. Chem. Soc.* **2009**, *131*, 3201−3209.
(8) Nederberg, F.; Lohmeijer, B. G. G.; Leibfarth, F.; Pratt, R. C.; Choi, J.; Dove, A. P.; Waymouth, R. M.; Hedrick, J. L. *Biomacromolecules* **2007**, *8*, 153−160.
(9) (a) Rodriguez, M.; Marrot, S.; Kato, T.; Stérin, S.; Fleury, E.; Baceiredo, A. *J. Organomet. Chem.* **2007**, *692*, 705−708. (b) Lohmeijer, B. G. G.; Dubois, G.; Leibfarth, F.; Pratt, R. C.; Nederberg, F.; Nelson, A.; Waymouth, R. M.; Wade, C.; Hedrick, J. L. *Org. Lett.* **2006**, *8*, 4683−4686.
(10) (a) Guo, L.; Lahasky, S. H.; Ghale, K.; Zhang, D. *J. Am. Chem. Soc.* **2012**, *134*, 9163−9171. (b) Guo, L.; Zhang, D. *J. Am. Chem. Soc.* **2009**, *131*, 18072−18074.
(11) (a) Coutelier, O.; El Ezzi, M.; Destarac, M.; Bonnette, F.; Kato, T.; Baceiredo, A.; Sivasankarapillai, G.; Gnanou, Y.; Taton, D. *Polym. Chem.* **2012**, *3*, 605−608. (b) Pinaud, J.; Vijayakrishna, K.; Taton, D.; Gnanou, Y. *Macromolecules* **2009**, *42*, 4932−4936. (c) Nyce, G. W.; Lamboy, J. A.; Connor, E. F.; Waymouth, R. M.; Hedrick, J. L. *Org. Lett.* **2002**, *4*, 3587−3590.
(12) (a) Webster, O. W. *Adv. Polym. Sci.* **2004**, *167*, 1−34. (b) Sogah, D. Y.; Hertler, W. R.; Webster, O. W.; Cohen, G. M. *Macromolecules* **1987**, *20*, 1473−1488. (c) Webster, O. W.; Hertler, W. R.; Sogah, D. Y.; Farnham, W. B.; RajanBabu, T. V. *J. Am. Chem. Soc.* **1983**, *105*, 5706−5708.
(13) Selected recent reviews and examples: (a) Fuchise, K.; Chen, Y.; Satoh, T.; Kakuchi, T. *Polym. Chem.* **2013**, *4*, 4278−4291. (b) Raynaud, J.; Liu, N.; Gnanou, Y.; Taton, D. *Macromolecules* **2010**, *43*, 8853−8861. (c) Raynaud, J.; Gnanou, Y.; Taton, D. *Macromolecules* **2009**, *42*, 5996−6005. (d) Raynaud, J.; Ciolino, A.; Baceiredo, A.; Destarac, M.; Bonnette, F.; Kato, T.; Gnanou, Y.; Taton, D. *Angew. Chem., Int. Ed.* **2008**, *47*, 5390−5393. (e) Scholten, M. D.; Hedrick, J. L.; Waymouth, R. M. *Macromolecules* **2008**, *41*, 7399−7404.
(14) Stephan, D. W.; Erker, G. *Angew. Chem., Int. Ed.* **2010**, *49*, 46−76.
(15) (a) Arduengo, A. J., III; Bock, H.; Chen, H.; Denk, M.; Dixon, D. A.; Green, J. C.; Herrmann, W. A.; Jones, N. L.; Wagner, M.; West, R. *J. Am. Chem. Soc.* **1994**, *116*, 6641−6649. (b) Arduengo, A. J., III; Dias, H. V. R.; Harlow, R. L.; Kline, M. *J. Am. Chem. Soc.* **1992**, *114*, 5530−5534.
(16) (a) Chen, E. Y.-X. *Top. Curr. Chem.* **2013**, *334*, 239−260. (b) Zhang, Y.; Miyake, G. M.; John, M. G.; Falivene, L.; Caporaso, L.; Cavallo, L.; Chen, E. Y.-X. *Dalton Trans.* **2012**, *41*, 9119−9134. (c) Zhang, Y.; Miyake, G. M.; Chen, E. Y.-X. *Angew. Chem., Int. Ed.* **2010**, *49*, 10158−10162.
(17) (a) Enders, D.; Breuer, K.; Kallfass, U.; Balensiefer, T. *Synthesis* **2003**, 1292−1295. (b) Enders, D.; Breuer, K.; Raabe, G.; Runsink, J.; Teles, J. H.; Melder, J.-P.; Ebel, K.; Brode, S. *Angew. Chem., Int. Ed.* **1995**, *34*, 1021−1023.
(18) Maji, B.; Breugst, M.; Mayr, H. *Angew. Chem., Int. Ed.* **2011**, *50*, 6915−6919.
(19) (a) Biju, A. T.; Padmanaban, M.; Wurz, N. E.; Glorius, F. *Angew. Chem., Int. Ed.* **2011**, *50*, 8412−8415. (b) Matsuoka, S.-I.; Ota, Y.; Washio, A.; Katada, A.; Ichioka, K.; Takagi, K.; Suzuki, M. *Org. Lett.* **2011**, *13*, 3722−3725.
(20) Zhang, Y.; Miyake, G. M.; Chen, E. Y.-X. *Angew. Chem., Int. Ed.* **2012**, *51*, 2465−2469.
(21) Recent reviews and examples: (a) Gowda, R. R.; Chen, E. Y.-X. *Encycl. Polym. Sci. Technol.* **2013**, DOI: 10.1002/0471440264.pst606. (b) Chen, X.; Caporaso, L.; Cavallo, L.; Chen, E. Y.-X. *J. Am. Chem. Soc.* **2012**, *134*, 7278−7281. (c) Shin, J.; Lee, Y.; Tolman, W. B.; Hillmyer, M. A. *Biomacromolecules* **2012**, *13*, 3833−3840. (d) Zhang, Y.; Gustafson, L. O.; Chen, E. Y.-X. *J. Am. Chem. Soc.* **2011**, *133*, 13674−13684. (e) Cockburn, R. A.; Siegmann, R.; Payne, K. A.; Beuermann, S.; McKenna, T. F. L.; Hutchinson, R. A. *Biomacromolecules* **2011**, *12*, 2319−2326. (f) Miyake, G. M.; Zhang, Y.; Chen, E. Y.-X. *Macromolecules* **2010**, *43*, 4902−4908. (g) Hu, Y.; Xu, X.; Zhang, Y.; Chen, Y.; Chen, E. Y.-X. *Macromolecules* **2010**, *43*, 9328−9336. (h) Miyake, G. M.; Newton, S. E.; Mariott, W. R.; Chen, E. Y.-X. *Dalton Trans.* **2010**, *39*, 6710−6718. (i) Juhari, A.; Mosnáček, J.; Yoon, J. A.; Nese, A.; Koynov, K.; Kowalewski, T.; Matyjaszewski, K. *Polymer* **2010**, *51*, 4806−4813.
(22) Hoffman, H. M. R.; Rabe, J. *Angew. Chem., Int. Ed. Engl.* **1985**, *24*, 94−110.
(23) (a) Manzer, L. E. *ACS Symp. Ser.* **2006**, *921*, 40−51. (b) Manzer, L. E. *Appl. Catal. A: Gen.* **2004**, *272*, 249−256.
(24) Maji, B.; Horn, M.; Mayr, H. *Angew. Chem., Int. Ed.* **2012**, *51*, 6231−6235.
(25) Knappke, C. E. I.; Arduengo, A. J., III; Jiao, H.; Neudörfl, J.-M.; Jacobi von Wangelin, A. *Synthesis* **2011**, 3784−3795.
(26) Breslow, R. *J. Am. Chem. Soc.* **1958**, *80*, 3719−3726.
(27) Fisher, C.; Smith, S. W.; Powell, D. A.; Fu, G. C. *J. Am. Chem. Soc.* **2006**, *128*, 1472−1473.
(28) Enders, D.; Breuer, K.; Teles, J. H.; Ebel, K. *J. Prakt. Chem.* **1997**, *339*, 397−399.
(29) DiRocco, D. A.; Oberg, K. M.; Rovis, T. *J. Am. Chem. Soc.* **2012**, *134*, 6143−6145.
(30) Berkessel, A.; Elfert, S.; Yatham, V. R.; Neudörfl, M.-M.; Schlörer, N. E.; Teles, J. H. *Angew. Chem., Int. Ed.* **2012**, *51*, 12370−12374.
(31) Such deoxy-Brewlow intermediates can also be formed from the reaction of NHC with alkyl halides,[25] two of which have also been structurally characterized later.[24]
(32) (a) Chen, E. Y.-X. *Chem. Rev.* **2009**, *109*, 5157−5214. (b) Baskaran, D.; Müller, A. H. E. *Prog. Polym. Sci.* **2007**, *32*, 173−219. (c) Rodriguez-Delgado, A.; Chen, E. Y.-X. *J. Am. Chem. Soc.* **2005**, *127*, 961−974. (d) Vlček, P.; Lochmann, L. *Prog. Polym. Sci.* **1999**, *24*, 793−873.
(33) Baskaran, D.; Müller, A. H. E. *Macromol. Rapid Commun.* **2000**, *21*, 390−395.
(34) Suenaga, J.; Sutherlin, D. M.; Stille, J. K. *Macromolecules* **1984**, *17*, 2913−2916.
(35) Flory, P. J. *Principles of Polymer Chemistry*, Cornell University Press: Ithaca, 1953.
(36) (a) Endo, K. *Adv. Polym. Sci.* **2008**, *217*, 121−183. (b) Roovers, J. In *Cyclic Polymers*, 2nd ed.; Semlyen, J. A., Ed.; Kluwer Academic: Dordrecht, The Netherlands, 2000; pp 347−384.
(37) Chu, Y.; Deng, H.; Cheng, J.-P. *J. Org. Chem.* **2007**, *72*, 7790−7793.
(38) Kim, Y.-J.; Streitwieser, A. *J. Am. Chem. Soc.* **2002**, *124*, 5757−5761.
(39) Odian, G. *Principles of Polymerization*, 4th ed.; John Wiley & Sons, Inc.: Hoboken, NJ, 2004; pp 238−255.
(40) All DFT calculations were performed using the Gaussian09 package. The Supporting Information contains details and references.
(41) (a) Poater, A.; Cosenza, B.; Correa, A.; Giudice, S.; Ragone, F.; Scarano, V.; Cavallo, L. *Eur. J. Inorg. Chem.* **2009**, 1759−1766. (b) Poater, A.; Ragone, F.; Giudice, S.; Costabile, C.; Dorta, R.; Nolan, S. P.; Cavallo, L. *Organometallics* **2008**, *27*, 2679−2681. (c) Cavallo, L.; Correa, A.; Costabile, C.; Jacobsen, H. *J. Organomet. Chem.* **2005**, *690*, 5407−5413.
(42) Hawkes, K. J.; Yates, B. F. *Eur. J. Org. Chem.* **2008**, 5563−5570.
(43) During the revision process of the present manuscript, the experimental mechanistic study of the TPT-catalyzed MMA dimerization just appeared: Kato, T.; Ota, Y.; Matsuoka, S.-I.; Takagi, K.; Suzuki, M. *J. Org. Chem.* **2013**, *78*, 8739−8747.